Arabian Journal of Geosciences (2021) 14: 2183
https://doi.org/10.1007/s12517-021-08569-z

ORIGINAL PAPER

Multi-analytical approach of provenance signatures and indication of marine environment in coal and shale bearing sequence from Makum Coalfield, India

Sanki Biswas[1] · Atul Kumar Varma[1] · Madhav Kumar[2] · Binoy K. Saikia[3]

Received: 13 August 2021 / Accepted: 1 October 2021 / Published online: 20 October 2021

Abstract
The well-developed coal and shale bearing sequence belong to the Tikak Parbat Formation (Oligocene) of the Makum Coalfield have been studied to understand the paleoclimate and depositional conditions through organic petrography, palynofacies, and mineralogy. The depositional settings of the studied formation range from mildly oxic-to-anoxic deltaic forest to limnic swamp environmental conditions. Both are marked by high vitrinite (~ 66.86 vol. %), with significant liptinites (7.26–34.46 vol. %) and low inertinite (≤ 4.77 vol. %). Similarly, palynofacies indicate high phytoclasts, with amorphous organic matter and few palynomorphs (mostly spores and pollens). These suggest dependence of higher plant organic matter (OM) on floral precursors likely controlled by the combination of depositional conditions, i.e., water level, temperature, salinity, etc. The dominance of terrestrial land plants as major OM source indicates high water level in the peat. In addition, the geochemical plot of MgO/Al_2O_3 and K_2O/Al_2O_3 and occurrences of framboidal pyrite and other carbonate mineral phase point towards non-marine to marine environment. The high K_2O and MgO in shales indicate periodic marine water incursion, perhaps due to sea-level rise. Samples mostly having 1–10 salinity and some have > 10 also specifies transitional environment. The inorganic matters (IM) within the sediments were mostly derived from mixed felsic igneous rocks of granodiorite and granite compositions and had experienced moderate-to-strong weathering which reveals change in climatic conditions during the Oligocene epoch. This study suggests existing of multiple phase environmental transformations during the deposition of coal and shale bearing sequence and further leads to the accumulation of diversified plant species and with sufficient basinal thermal maturity.

Keywords Makum Coalfield · Maceral; Mineralogy · Paleoenvironment · Weathering index

Introduction

The Tikak Parbat Formation (younger part of the Barial Group) in the Makum Coalfield of the Upper Assam Basin of India has become a research interest for many scientists as the formation contains thick coal and shale beds in the younger part of the Barial Group (Raja Rao, 1981; Ahmed, 1996; Biswas et al. 2020). The basin is also long been known as one of the major onshore petroleum-producing regions of India and the bulk of the oil production is from clastic reservoirs belonging to the Barail (Oligocene) and Tipam (Miocene) formations (Mathur and Evans, 1964; Raju, 1968; Bhandari et al. 1973; Handique and Bharali, 1981; Ranga, 1983; Raju and Mathur, 1995; Naidu and Panda, 1997; Mathur, 2014). Earlier works, like Chandra et al. (1984), Goswami (1985), Misra (1992), Ahmed (1996), Mishra and Ghosh (1996), Rajarathnam et al. (1996), and Saikia et al. (2014, 2015, and 2016), have studied the Oligocene coal and carbonaceous shale of the Tikak Parbat Formation (uppermost formation of the Barail Group) and reported the physical properties, chemical attributes, and petrographic assemblages. Kumar et al. (2012) and Srivastava et al.

Responsible Editor: Santanu Banerjee

✉ Sanki Biswas
sanki2810@gmail.com

[1] Coal Geology and Organic Petrology Laboratory, Dept. of Applied Geology, Indian Institute of Technology (Indian School of Mines), Dhanbad, India

[2] Birbal Sahni Institute of Palaeosciences, Lucknow, India

[3] Polymer Petroleum and Coal Chemistry Group (MSTD), CSIR—North East Institute of Science and Technology, Jorhat, Assam, India

(2012) have studied the detailed composition of the plant communities, their spreading, climatic conditions (temperature), and precipitation parameters of the organic sediments from the Tirap colliery via sedimentology, palynofacies, and pollen and spore assemblages study. They have pointed out that the lower part of the Tikak Parbat Formation represents a lower delta-plain environment, whereas the uppermost part of the formation is suggestive of an upper delta-plain environment. Similarly, based on the biomarker signature, Rudra et al. (2017) also reported changes in vegetation, the dominance of gymnosperms during the early Paleogene to the presence of angiosperms in the Eocene. The organic matter (OM) is dominant of terrestrial and waxy plant material and was deposited within fluvio-deltaic and anoxic depositional environments. Gogoi et al. (2008) and Sharma et al. 2018) inferred that coal and shale have a mixture of type III (predominant) and type II OM and exhibit very good source rock quality. Recently, Biswas et al. (2020) have discussed the hydrocarbon generation potential of the Makum coal and shale, and pointed out that they have the potential to generate mixed thermogenic gas and condensate oil. The occurrences of the gas within the coal and shale are mainly controlled by various geological factors, such as depositional conditions and tectonic settings of that area (Dai et al. 2020).

The sedimentary organic matter (OM) contains a detailed geological record of past environmental conditions and geodynamic indicators, and these further lead to understanding the occurrence of thermogenic gas and oil in coal and shale litho-units. The identification of OM through petrography and palynofacies provides vital information to trace out the source, OM accumulation, and their associated depositional conditions (Stach et al. 1982; Teichmüller, 1989; Taylor et al. 1998; Moore and Shearer, 2003; Suárez-Ruiz et al. 2012; Varma et al. 2019; Biswas, 2021). Similarly, mineralogical parameters are incorporated to better understand the degree of weathering, paleotectonic setting, and paleoenvironmental conditions (Nesbitt and Young, 1982, 1984; Bhatia, 1983; Dickinson et al. 1983; Roser and Korsch, 1988; Condie, 1993; Nesbitt et al. 1996; Hayashi et al. 1997; Ward, 2002; Shehata and Abdou, 2008; Dai et al. 2016; Zhao et al. 2017). These multi-proxies are combined and assessed to understand the provenance and depositional conditions of the OM in the coal and shale bearing sequence belong to the Tikak Parbat Formation (Oligocene) of the Makum Coalfield, India. The detailed mineralogical parameters obtained from the X-ray fluorescence (XRF) and X-ray diffraction (XRD) analyses are being published for the first time and the data are correlated with the petrography and palynofacies assemblages (from Biswas et al. 2020) to fulfill the objectives of the research goals (following Stach et al. 1982; Teichmüller, 1989; Lamberson et al. 1991; Alkande et al. 1992; Diessel, 1992; Crosdale, 1993; Dehmer, 1993; Tyson, 1995; Batten, 1996a, b; Taylor et al. 1998; Wüst et al. 2001; Scott, 2002; Moore and Shearer, 2003; Silva and Kalkreuth, 2005; Mendonça Filho et al. 2011, 2012). The outcomes from this study will aid in better understanding the accumulation and preservation of the organic matters in transitional environment conditions. This study is also of significance to estimating the source rock potential in the Makum Coalfield.

Geological setting and sampling area

The Makum Coalfield of Assam is one of the economically significant Tertiary coalfields of Northeast India (located between 27° 15′ N and 27° 25′ N; 95° 40′ E and 95° 55′ E; Fig. 1), and encompasses an approximate coal reserve of 452.79 million tonnes (IBM, 2019). The organics and sediments comprising coal and shale were deposited along linear, active thrust belts that are demarcated by numerous overthrusts, known as the "Belt of Schuppen" (Mathur and Evans, 1964). Furthermore, the coal/shale bearing strata have experienced ductile deformation and were folded to form an asymmetrical syncline (Mathur and Evans, 1964). Structures that resulted from deformation have also been preserved within individual coal beds (Francis, 1961; Stach et al. 1982; Ahmed, 1989, 1996). The detailed geological work in the coalfield has been carried out by Meddlicott (1865) and Mallet (1876). Based on the lithological characteristics, Evans (1932) subdivided the Oligocene sediments of the Barail Group into the Naogaon, Baragolai, and Tikak Parbat formations. The thick coal and shale strata are mainly reported from the Tikak Parbat Formation and this unit is known as the "Coal Measure Sub Series" (Mallet, 1876). The Tikak Parbat Formation is 300 to 600 m thick and is composed of sandstone, mudstone, carbonaceous shale, coal, claystone, and siltstone. The underlying Baragolai Formation, which has a thickness of approximately 300 m, consists of massive, micaceous, or ferruginous sandstone, with alteration of claystone, mudstone, carbonaceous shale units, and thin coal layers. The bottommost formation, i.e., the Naogaon Formation (1100 to 1700 m thick), contains fine-grained, thin-bedded quartzitic sandstones, and thin layered shales (Mishra and Ghosh, 1996). The patchy occurrence of dolomitic limestones within the formation has also been reported by Misra (2000).

The studied Oligocene Tikak Parbat Formation (uppermost formation of the Barail Group) of the Makum Coalfield contains five coal seams, and out of them, 60, 20, and 8 ft seams (names of the coal seams) are under working conditions (GSI (Geological Survey of India), 2009). Besides coal seams, the formation is also known to have five thick shale horizons (Biswas et al. 2020 and Biswas, 2021). As the studied horizons were not completely accessible in all the mines during the time of sampling, thus, to accomplish the objectives, we have systematically collected samples from four

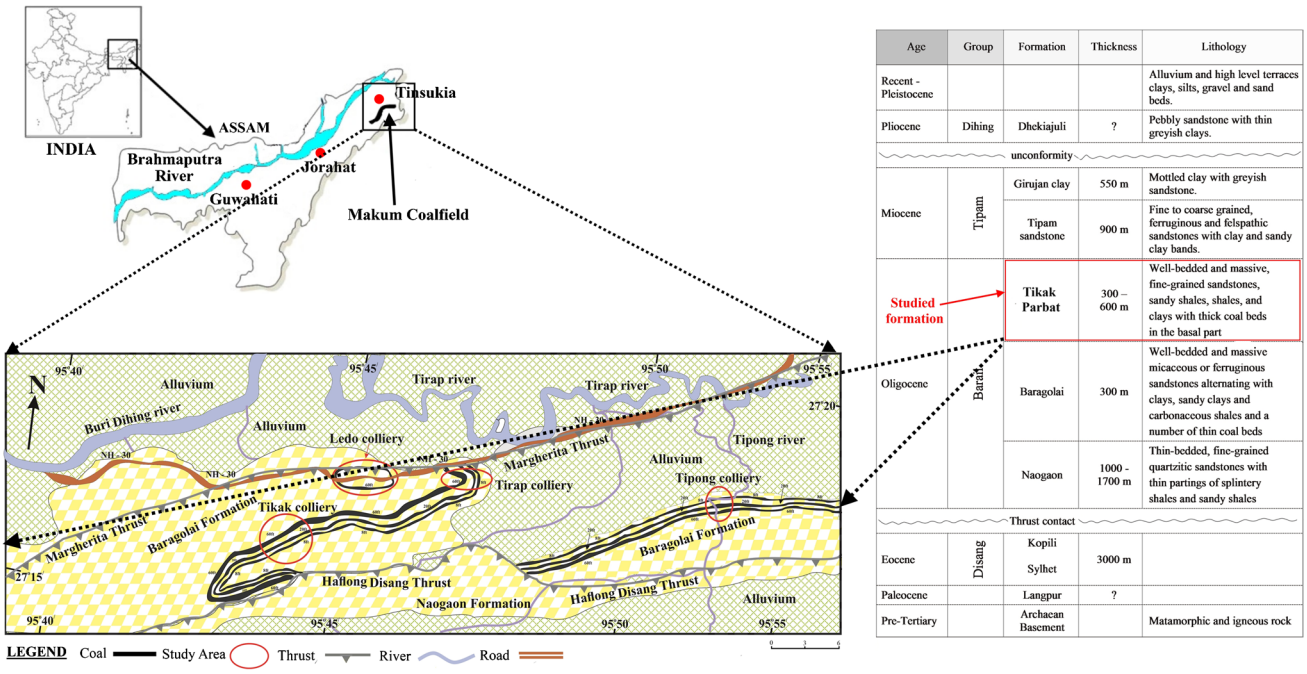

Age	Group	Formation	Thickness	Lithology
Recent - Pleistocene				Alluvium and high level terraces clays, silts, gravel and sand beds.
Pliocene	Dihing	Dhekiajuli	?	Pebbly sandstone with thin greyish clays.
unconformity				
Miocene	Tipam	Girujan clay	550 m	Mottled clay with greyish sandstone.
		Tipam sandstone	900 m	Fine to coarse grained, ferruginous and felspathic sandstones with clay and sandy clay bands.
Oligocene	Barail	Tikak Parbat (Studied formation)	300 – 600 m	Well-bedded and massive, fine-grained sandstones, sandy shales, shales, and clays with thick coal beds in the basal part
		Baragolai	300 m	Well-bedded and massive micaceous or ferruginous sandstones alternating with clays, sandy clays and carbonaceous shales and a number of thin coal beds
		Naogaon	1000 - 1700 m	Thin-bedded, fine-grained quartzitic sandstones with thin partings of splintery shales and sandy shales
Thrust contact				
Eocene	Disang	Kopili Sylhet	3000 m	
Paleocene		Langpur	?	
Pre-Tertiary		Archaean Basement		Matamorphic and igneous rock

Fig. 1 Geology map and generalized lithostratigraphic succession of the Makum Coalfield, Assam, India, showing the study area and sample locations (slightly modified Raja Rao, 1981; Ahmed, 1996; Biswas et al. 2020)

different mines, that is, the Ledo, Tirap, Tikak, and Tipong collieries. Out of the twenty samples, seven were sampled from the Tipong colliery, five samples from the Tikak colliery, five samples from the Tirap colliery, and the remaining three from the Ledo colliery. Each sample represents the corresponding lithology from which it has been collected (Fig. 2). To avoid alteration or contamination, samples were taken after removing at least 10 to 15 cm of the exposed part. They were dried in the air, crushed, and were prepared for XRF and XRD analysis and for micropetrography and palynofacies.

Materials and methods

X-ray fluorescence (XRF)

The oxide concentrations were detected by XRF analysis and are exhibited in Table 1. The Rikako Koyama XRF instrument was used to analyze samples at the Research and Development Centre for Iron and Steel (RDCIS), in Ranchi, India. For the analysis, crushed samples of 75 µm size were taken after coning and quartering, and they were burned at 850 °C. Then 5 g of the residue was retrieved, and to make it compact, one to two drops of paraffin were mixed thoroughly with it. After that, it was pressed by a 20 tonnes weight for about 1 min within a pressing machine. The prepared pellets were covered by 1-micron mylar foil and kept inside the XRF machine for conducting the analysis.

X-ray diffraction (XRD)

The mineralogical assemblages present in the source rock were determined through XRD analysis. Dry powdered samples were analyzed by using a PANalytical X′pert PRO Diffractometer and the outcome is shown in Table 2. The scanning was performed at a 2θ range of 5 to 119°, with a scanning time of 2° per minute and 0.0170° step size. The XRD curves were interpreted by using the High Score Plus software package and were correlated with the ICDD (International Centre for Diffraction Data) database to document the crystalline mineral phases (ICDD, 2011; Silva et al. 2011a, b).

Petrographic study

A “Leica DM2700 P” microscope with an oil immersion lens and attached fluorescence was used for maceral analysis at the Coal Geology and Organic Petrology Lab., Dept. of Applied Geology, Indian Institute of Technology (Indian School of Mines), in Dhanbad, India. The polished pellets were prepared with the < 1-mm size crushed samples following the specifications of ISO (2009a, b, c), and the macerals were classified following ICCP (1998, 2001) and Pickel et al. (2017). More than 1000 points were counted

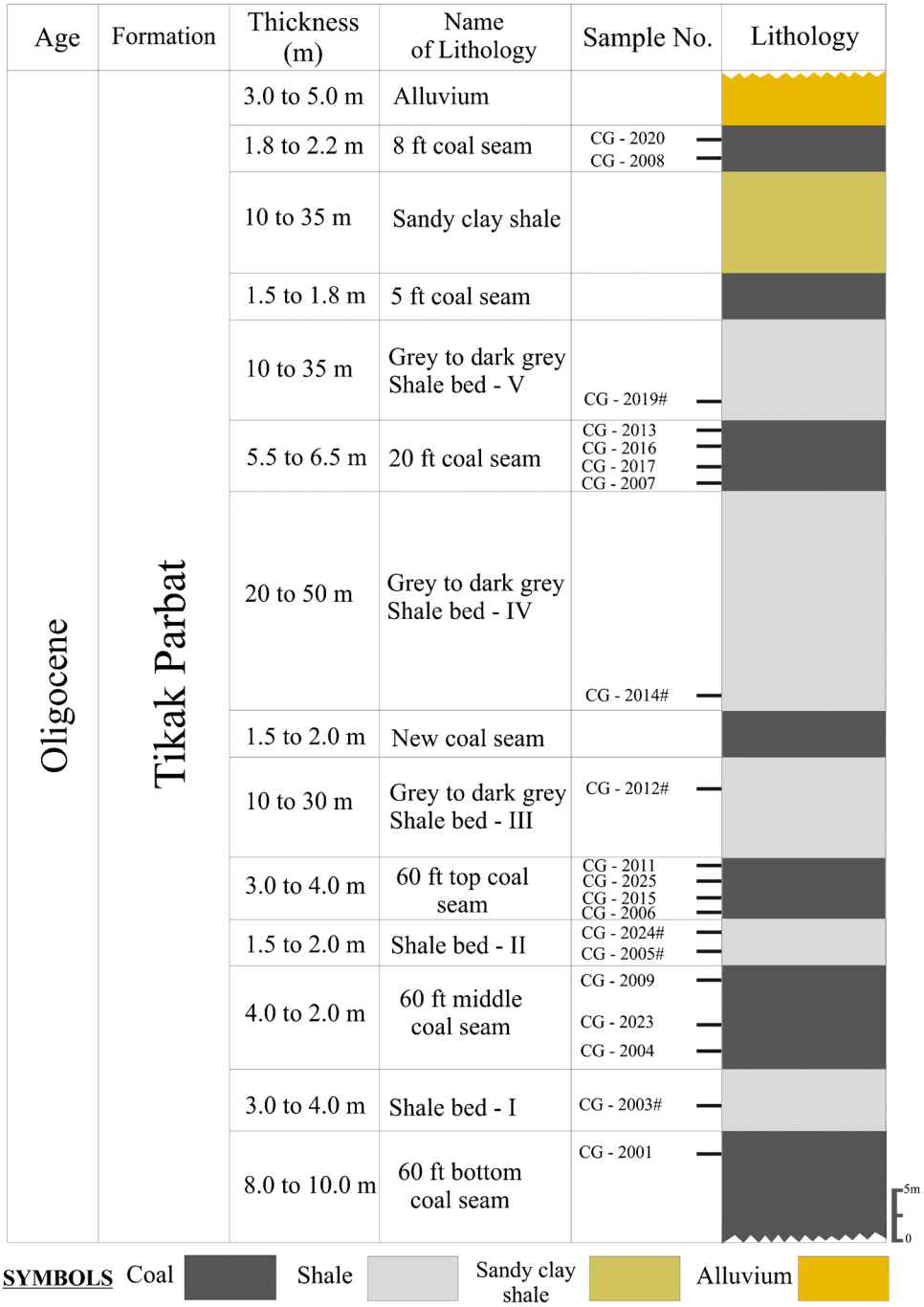

Fig. 2 The distribution of samples within the coal and shale beds from Makum Coalfield, Assam, India

via use of a point counter for each pellet. The total maceral content (TMC) was calculated from the sum of all the macerals counted by following Stach et al. (1982) and Taylor et al. (1998). Additionally, the vitrinite reflectance (R_o) was measured with the help of PMT III and MSP 200 software using the same pellet (following ASTM, 1994). One hundred collotelinite grains, which were homogeneous and free of impurities, were selected to measure the R_o values (ISO, 2009c). The calibration was done with the leucosapphire (0.594) standard before the analysis. The detailed maceral composition and corresponding reflectance values are shown in Table 3.

Palynofacies study

The cleaned and crushed coal and shale samples were treated with 40% hydrochloric (HCl) for 6 h and 70% hydrofluoric (HF) acid for 12 h to dissolve the carbonates and silicates, respectively (Traverse, 1988). To remove the humic material, the residual samples were treated again

Table 1 Results of oxide distributions (wt. %) and various geochemical indices of the studied samples from the Makum Coalfield, Assam, India

Area	Lithology	Sequence No	Sample number	SiO_2	Al_2O_3	Fe_2O_3	K_2O	CaO	MgO	TiO_2	P_2O_5	Na_2O	SO_3	CIA	CIW	K_2O/Al_2O_3	Na_2O/Al_2O_3	MgO/Al_2O_3	K_2O/Na_2O	Al_2O_3/TiO_2	A^d	FC	S^{daf}
Tirap	8-ft coal seam	MC 1	CG 2020	38.18	30.57	20.79	0.07	0.59	1.41	1.03	0.01	1.51	5.84	93.37	93.56	0.002	0.049	0.046	0.050	29.71	10.80	43.80	8.30
Tipong	8-ft coal seam	MC 2	CG 2008	55.76	31.63	9.01	0.09	0.35	0.24	1.04	0.02	0.74	1.12	96.39	96.67	0.003	0.023	0.007	0.130	30.53	6.00	53.50	2.12
Tirap	Shale bed-V	MS 3	CG 2019#	61.87	25.06	7.24	2.73	0.34	0.80	0.71	0.08	0.35	0.83	87.98	97.31	0.109	0.014	0.032	7.720	35.30	73.30	10.10	17.73
Tirap	20-ft coal seam	MC 5	CG 2016	35.16	28.28	17.49	1.78	1.66	2.34	1.81	0.10	6.86	4.52	73.31	76.85	0.063	0.243	0.083	0.260	15.63	2.30	50.50	8.29
Tirap	20-ft coal seam	MC 6	CG 2017	35.33	30.59	17.77	1.48	1.69	2.51	1.31	0.10	5.89	3.33	77.15	80.14	0.048	0.193	0.082	0.250	23.34	4.00	51.30	7.97
Tipong	20-ft coal seam	MC 7	CG 2007	52.55	28.04	11.03	0.71	1.19	3.26	1.33	0.09	0.91	0.88	91.73	93.90	0.025	0.032	0.116	0.780	21.10	1.00	53.70	6.16
Tikak	Shale bed-IV	MS 8	CG 2014#	60.58	26.49	7.93	2.11	0.22	0.46	0.60	0.08	0.26	1.27	91.10	98.24	0.080	0.010	0.017	8.170	44.15	34.90	30.90	10.46
Tikak	Shale bed-III	MS 9	CG 2012#	64.06	23.59	5.52	2.47	0.84	1.61	0.52	0.18	0.60	0.61	86.52	95.13	0.105	0.026	0.068	4.090	45.37	86.10	2.90	5.99
Tirap	60-ft top coal seam	MC 12	CG 2015	41.10	26.33	15.14	0.62	3.93	2.00	1.68	0.15	5.20	3.85	72.97	74.24	0.023	0.197	0.076	0.120	15.64	2.00	55.60	2.39
Ledo	Shale bed-II	MS 14	CG 2024#	63.88	24.37	5.92	2.33	0.70	1.52	0.38	0.16	0.33	0.41	89.09	97.39	0.096	0.013	0.062	7.150	64.13	86.50	1.20	5.15
Tipong	Shale bed-II	MS 15	CG 2005#	59.90	24.72	7.84	2.61	0.51	2.22	0.56	0.09	0.32	1.24	88.42	97.51	0.105	0.013	0.090	8.240	44.14	82.00	4.90	19.03
Tikak	60-ft middle coal seam	MC 16	CG 2009	49.02	29.69	10.53	0.27	2.88	5.01	1.21	0.03	0.43	0.93	96.35	97.18	0.009	0.014	0.169	0.620	24.47	2.00	52.00	1.89

Table 1 (continued)

Area	Lithology	Sequence No	Sample number	SiO_2	Al_2O_3	Fe_2O_3	K_2O	CaO	MgO	TiO_2	P_2O_5	Na_2O	SO_3	CIA	CIW	K_2O/Al_2O_3	Na_2O/Al_2O_3	MgO/Al_2O_3	K_2O/Na_2O	Al_2O_3/TiO_2	A^d	FC	S^{daf}
Ledo	60-ft middle coal seam	MC 17	CG 2023	56.78	29.55	5.58	0.19	1.72	1.76	1.13	0.22	1.59	1.49	89.76	90.28	0.006	0.054	0.060	0.120	26.23	2.30	54.50	1.92
Tipong	Shale bed-I	MS 19	CG 2003#	69.06	24.15	2.01	2.26	0.35	0.77	0.61	0.06	0.28	0.44	89.55	97.74	0.094	0.012	0.032	8.100	39.59	88.30	3.20	1.83
Tipong	60-ft bottom coal seam	MC 20	CG 2001	54.03	26.08	8.64	0.26	2.80	4.78	1.19	0.04	1.62	0.56	88.16	88.95	0.010	0.062	0.183	0.160	21.94	4.16	51.93	1.27

Explanations: #=shale; CIA (chemical index of alteration)=$[Al_2O_3/(Al_2O_3+CaO^*+Na_2O+K_2O)]\times100$; CIW (chemical index of weathering)=$[Al_2O_3/(Al_2O_3+CaO^*+Na_2O)]\times100$; *A*: ash yield (wt. %); *FC*: fixed carbon (wt. %); *S*: sulfur (wt. %); *d*: dry basis; *daf*: dry ash free basis. Note: The values of ash yield, fixed carbon, and sulfur content of the same samples have been taken from Biswas et al. 2020

with 60% nitric acid (HNO_3). The washed residues were further nursed once again to dispel the silico-fluoride with the help of dilute HCl. After maceration, the remaining samples were used to prepare slides (following Batten, 1996a, 1999; Batten and Stead, 2005). The slides were investigated underneath the petrographic microscope and at least 500 counts organic matter were conducted for quantitative analysis and were also used to interpret OM type within the peat swamps and their respective paleodepositional environmental conditions (Tyson, 1995; Batten, 1996a; Mendonça Filho et al. 2002, 2010, 2011, 2012; Batten and Stead, 2005; Carvalho et al. 2006). The volumetric percentages (vol. %) of the identified OM are listed in Table 4.

Results

Geochemistry

Oxide distribution

The oxide compositions exhibit that SiO_2 is the most abundant oxide varying between 35.16 and 55.76 wt. % in coal and that in shale ranges from 59.90 to 69.06 wt. % (Table 1). The second most abundant oxide, Al_2O_3, ranges from 26.08 to 31.63 and 23.59 to 26.49 wt. % in coal and shale, respectively. And the third, Fe_2O_3, varies from 5.58 to 20.79 in coal samples and 2.01 to 7.93 wt. % in shale samples. In addition to the three major oxides present in the samples, there are also minor oxides, such as CaO, MgO, TiO_2, K_2O, P_2O_5, SO_3, and Na_2O. Furthermore, the chemical index of alteration (CIA) and chemical index of weathering (CIW) have been assessed from the compilation of oxide compositions in order to forecast the paleoclimatic conditions associated with deposition (Nesbitt and Young, 1982; Harnois, 1988). The equations are as follows:

$$CIA = \{Al_2O_3 \times 100/(Al_2O_3 + C_aO^*Na_2O + K_2O)\} \quad (1)$$

$$CIW = \{Al_2O_3 \times 100/(Al_2O_3 + C_aO^*Na_2O)\} \quad (2)$$

Here, CaO* is obtained from the method provided by Bock et al. (1998). According to the methodology, if Na_2O is smaller than CaO, then $Na_2O = CaO^*$, or otherwise $CaO = CaO^*$ value.

The CIA and CIW indices range from 72.97 to 96.39 (avg. 86.58) and 74.24 to 97.18 (avg. 87.98) in coal samples, and 86.52 to 89.55 (avg. 88.78) and 95.13 to 98.24 (avg. 97.22) in shale, respectively (Table 1).

Table 2 Minerals identified by XRD in the high-temperature ash samples from the Makum Coalfield, India

Sequence no	Sample number	Identified minerals
MC 2	CG 2008	Quartz (m), berlinite (w), wollastonite/(quartz + calcite) (m), microcline (m), lucite (w), corundum (m), spinel (w)
MS 3	CG 2019#	Quartz (s), feldspar (m), berlinite (m), pyrite (w), kaolinite (m)
MC 5	CG 2016	Quartz (m), feldspar (m), berlinite (w), wollastonite/(quartz + calcite) (m)
MS 9	CG 2012#	Quartz (m), wollastonite/(quartz + calcite) (m), microcline (m)
MC 12	CG 2015	Quartz (m), berlinite (w), microcline (w), spinel (w), nepheline (vs)
MS 15	CG 2005#	Quartz (m), wollastonite/(quartz + calcite) (m), microcline (w), corundum (w), diopside (w), magnetite (w)
MC 16	CG 2009	Quartz (m), berlinite (w), wollastonite/(quartz + calcite) (m), magnetite (w)
MS 19	CG 2003#	Quartz (m), berlinite (w), wollastonite/(quartz + calcite) (m), microcline (m), lucite (w), mullite (w)
MC 20	CG 2001	Quartz (m), berlinite (w), wollastonite/(quartz + calcite) (m), microcline (vs), lucite (w), spinel (w), mullite (w)

Explanations: The relative XRD intensity is indicated within bracket (); *vs:* very strong; *s:* strong; *m:* moderate; and *w:* weak; # = shale

Table 3 Maceral and mineral matter distribution (vol. %) of the studied samples from the Makum Coalfield, Assam, India

Sequence no	Sample number	V	L	I	TMC	Clay	Pyrite	OMM	T_{MM}	Romv
MC 1	CG 2020	52.73	22.26	1.48	76.47	6.59	7.12	9.82	23.51	0.48
MC 2	CG 2008	56.44	16.67	2.67	75.78	5.53	2.11	16.58	24.22	0.38
MS 3	CG 2019#	9.89	10.95	*	20.84	3.89	4.95	70.32	79.16	0.41
MC 4	CG 2013	52.24	28.85	2.57	83.66	2.88	0.96	12.5	16.34	0.56
MC 5	CG 2016	51.06	33.10	0.70	84.86	1.41	2.11	11.62	15.14	0.50
MC 6	CG 2017	55.24	27.83	0.52	83.59	3.27	5.16	7.98	16.41	0.47
MC 7	CG 2007	43.43	31.87	2.39	77.69	9.90	1.99	10.52	22.41	0.51
MS 8	CG 2014#	30.80	13.08	1.27	45.15	10.55	5.49	38.83	54.87	0.48
MS 9	CG 2012#	13.05	14.33	*	27.38	21.98	3.87	46.77	72.62	0.51
MC 10	CG 2011	49.99	32.82	3.44	86.25	1.91	1.15	10.69	13.75	0.41
MC 11	CG 2025	44.90	34.46	1.00	80.36	2.37	2.69	14.57	19.63	0.46
MC 12	CG 2015	57.54	28.57	0.40	86.51	2.38	1.19	9.92	13.49	0.48
MC 13	CG 2006	63.66	16.24	4.06	83.96	4.06	3.85	8.13	16.04	0.46
MS 14	CG 2024#	5.70	7.72	*	13.42	11.41	1.68	73.49	86.58	0.52
MS 15	CG 2005#	7.27	7.26	*	14.53	5.51	6.02	73.94	85.47	0.51
MC 16	CG 2009	59.76	21.67	1.90	83.33	2.28	2.53	11.87	16.68	0.42
MC 17	CG 2023	66.86	15.22	0.36	82.44	3.99	0.50	13.07	17.56	0.52
MC 18	CG 2004	66.39	16.27	0.72	83.38	2.62	3.48	10.52	16.62	0.43
MS 19	CG 2003#	5.58	8.85	0.33	14.76	2.60	1.33	81.31	85.24	0.62
MC 20	CG 2001	60.08	21.47	4.47	86.02	2.69	2.40	8.89	13.98	0.49

Explanations: # = shale; V: total vitrinite group of macerals; I: total inertinite group of macerals; L: total liptinite group of macerals; *TMC:* total maceral content (vol. %); *OMM:* other minerals; *TMM:* total mineral matters (TMM = clay + pyrite + other minerals); Romv: mean vitrinite (collotelinite) reflectance (%); *traces. Note: Data in analytical basis and taken from Biswas et al. (2020)

Mineralogical compositions

The identified minerals through XRD diffractograms indicate that the samples (coal and shale) are possibly composed of quartz, wollastonite, nepheline, magnetite, spinel, corundum, berlinite, and mullite (Table 2). The peaks of kaolinite and pyrite are not present in the spectrum as they occur at low temperatures. Pyrite undergoes oxidation at 370 °C. It has also been pointed out that the calcite peaks are not detected in the diffractograms, but wollastonite is commonly present in the samples in a large percentage. This might be due to the chemical reaction between calcite ($CaCO_3$) with silica/quartz (SiO_2) in the formation of wollastonite ($CaSiO_3$), which took place at high temperature (750 to 900 °C). The hydrothermal reaction is as follows:

$$CaCO_3 + SiO_2 = CaSiO_3 + CO_2$$

Table 4 Distribution of organic matter based on palynofacies analysis (vol. %)

Sequence no	Sample number	Phytoclasts				T_{phy}	Amorphous organic matter		T_{AOM}	Palynomorphs		T_{pal}
		Cut	Wd	BioD	Bd		AOM	Re		Spo	Ff	
MC 1	CG 2020	2.93	1.02	71.70	0.78	76.43	8.66	11.59	20.24	3.33	0.19	3.33
MC 2	CG 2008	4.10	1.85	66.44	1.28	73.67	10.81	12.38	23.19	2.21	0.24	3.14
MS 3	CG 2019#	3.93	1.55	77.58	0.79	83.85	5.11	9.02	14.12	2.03	*	2.03
MC 4	CG 2013	3.42	1.10	60.15	*	64.67	6.91	24.05	30.97	3.53	2.00	4.37
MC 5	CG 2016	5.35	1.42	65.59	0.81	73.17	9.43	13.86	23.29	3.55	0.76	3.55
MC 6	CG 2017	5.45	1.84	64.96	0.79	73.04	11.42	12.65	24.07	2.89	0.84	2.89
MC 7	CG 2007	4.59	1.52	57.15	1.31	64.57	19.99	10.30	30.28	4.74	0.53	5.14
MS 8	CG 2014#	4.96	0.53	71.23	1.30	78.02	8.23	12.02	20.25	1.73	*	1.73
MS 9	CG 2012#	4.33	*	69.75	2.60	76.68	12.42	8.97	21.39	1.93	*	1.93
MC 10	CG 2011	2.70	*	69.71	1.54	73.95	10.61	11.20	21.81	4.24	*	4.24
MC 11	CG 2025	2.47	1.21	61.59	1.13	66.39	10.79	19.73	30.52	3.09	*	3.09
MC 12	CG 2015	4.59	1.06	61.96	2.57	70.18	15.17	10.67	25.84	3.72	0.62	3.98
MC 13	CG 2006	3.11	0.91	67.90	2.21	74.13	10.36	13.93	24.29	1.39	*	1.58
MS 14	CG 2024#	2.15	0.32	70.76	2.17	75.40	12.74	8.82	21.55	3.04	*	3.04
MS 15	CG 2005#	4.94	0.60	75.65	*	81.19	13.33	4.79	18.12	0.70	*	0.70
MC 16	CG 2009	2.56	0.55	78.44	3.89	85.43	1.77	10.25	12.01	2.04	0.67	2.56
MC 17	CG 2023	4.14	1.13	69.98	0.32	75.57	13.36	9.79	23.16	2.55	0.78	2.55
MC 18	CG 2004	5.22	1.10	56.62	1.57	64.52	26.74	4.93	31.67	2.67	*	3.81
MS 19	CG 2003#	1.67	0.51	75.50	5.33	83.01	12.22	2.40	14.63	1.20	0.75	2.36
MC 20	CG 2001	6.36	1.70	56.24	2.20	66.50	27.14	2.49	29.63	2.75	0.34	3.87

Explanations: #=shale; *Cut:* cuticle; *Wd:* wood; *BioD:* biodegraded; *Bd:* black debris; T_{phy}: total amount of phytoclasts; *AOM:* amorphous organic matter; *Re:* resin; $T_{AOM:}$ total amount of amorphous organic matter; *Spo:* sporomorphs; *Ff:* fungal filament; T_{pal}: total amount of palynomorphs; *traces. Note: Data are taken from Biswas et al. 2020

Petrographic assemblages

The identified macerals are very significant for understanding the paleoenvironmental and paleoclimatic conditions of the organic and inorganic matter deposition. Maceral distributions suggest that OM present in coal and shale are dominantly vitrinite macerals (43.33 to 66.86 vol. % in coal; 5.58 to 30.80 vol. % in shale) having the majority of collotelinite, and some amount of vitrodetrinite, collodetrinite, corpogelinite, gelinite, and telinite. Similarly, liptinites in the range of 15.22 to 34.46 in coal and that in the shale vary from 7.26 to 14.33 vol. % (Table 3). Among them, resinite, liptodetrinites, bituminite, and alginite are abundant, while sporinite, cutinite, suberinite, and exsudatinite are less abundant. Besides vitrinite and liptinite, samples also possess minor inertinite (0.36–4.77 vol. % in coal and 0.33–1.27 vol. % in shale). Within the inertinite macerals, inertodetrinite is the dominant macerals, while funginite and micrinites occur in a small percentage. The mean reflectance (Romv) value for the coal and shale ranges from 0.38 to 0.56% and 0.41 to 0.62%, separately. Study of such sample results more or less immature, but some are in close proximity to the oil generation zone.

Palynofacies

The OM retrieved from the samples (coal and shale) is dominated by phytoclasts, with some amount of amorphous OM (AOM) and palynomorphs (following Tyson, 1995; Batten, 1996a, b; Mendonça Filho et al. 2011, 2012). These OM are important to better understand the proximal-to-distal deposition conditions of the coalfield. The phytoclasts are subdivided into (1) non-opaque [cuticles, wood, and biodegraded], (2) opaque phytoclasts (black debris), and (3) palynomorphs, which are further partitioned into spores, pollen, and fungal bodies or filaments. Likewise, AOM includes bacteria-derived or biodegraded OM, diagenetic products of macrophyte tissues, and resins from higher plants.

Phytoclasts are 125- to 250-μm-sized fragments of higher land plants that range from 64.52 to 85.43 and 75.40 to 83.85 vol. % in coal and shale, respectively (Table 4). Among phytoclasts group of organic matter, non-opaque phytoclast (avg. 70.13 and 77.66 vol. %) shows dominance over the opaque (avg. 1.46 and 2.44 vol. %) phytoclasts in both coal and shale. Furthermore, biodegraded OM under non-opaque phytoclasts are abundance (avg. coal: 64.89; shale: 73.41 vol. %), whereas cuticles (avg. coal: 4.07; shale: 3.66 vol. %)

and wood (avg. coal: 1.26; shale: 0.70 vol. %) particles are found in a small amount. The AOM formed due to bacterial and fungal degradation ranges from 12.01 to 31.67 and 14.12 to 21.55 vol. % in coal and shale, respectively (Table 4). Among the three major OM groups, palynomorphs are the least concentrated and vary from 1.57 to 4.37 vol. % in coal and 0.70 to 3.04 vol. % in shale (Table 4). The documented palynomorphs are mainly of fern spores and angiosperm pollen grains (Tyson, 1995; Mendonça Filho et al. 2011). However, the authors have not recognized and categorized the palynomorphs genera in this study.

Discussion

Origin of inorganic matter and paleodepositional environment

The oxide compositions of the inorganic constituents provide valuable information about the source of the inorganic matter, as well as the affinity, paleoclimatic conditions, degree of weathering, and paleotectonic setting of the area (Nesbitt and Young, 1982, 1984; Bhatia, 1983; Dickinson et al. 1983; Roser and Korsch, 1988; Condie, 1993; Nesbitt et al. 1996; Hayashi et al. 1997; Ward, 2002; Shehata and Abdou, 2008; Dai et al. 2016; and Zhao et al. 2017). The presence of a large amount of SiO_2 and Al_2O_3 implies the occurrence of a significant amount of aluminosilicate minerals in both coal and shale (Table 1). Samples with a higher percentage of Fe_2O_3 might be due to abundant pyrites and other iron-bearing minerals. The low CaO content indicates a small amount of calcite minerals in the samples. Inspection of high TiO_2 values suggests that the inorganic sediments within the coal and shale are closely associated with basaltic rock composition (Dai et al. 2005; Chi and Yan, 2007). Furthermore, to investigate the source of clay minerals associated with organic matters, a TiO_2 vs Al_2O_3 diagram was plotted (Fig. 3). The diagram shows that the clay minerals mainly originate from felsic igneous rocks through chemical weathering processes (Amajor, 1987; Imchen et al. 2014). We have also calculated the Al_2O_3/TiO_2 ratios and observed most of the samples possessing Al_2O_3/TiO_2 ratios greater than 21 (except two coal samples, i.e., CG, 2015; and CG, 2016; see Table 1). This signifies the dominance of felsic igneous rocks in the source sediment (Dai et al. 2016; Zhao et al. 2017). The positive correlation of K_2O with ash yield ($r^2 = 0.84$) also exhibits the felsic source of the sediments. Presence of a significant amount of Fe_2O_3 and MgO in the samples suggests, however, the occurrence of some mafic minerals. Also, to determine the organic affinity of the oxides, correlation coefficient was calculated following Pearson's algorithm. The correlations show that various oxides, that is to say Al_2O_3, CaO, Fe_2O_3, Na_2O, SO_3, TiO_2, and MgO, are positively correlated with the fixed carbon (FC) under proximate analysis, having $r^2 = 0.80$, 0.60, 0.58, 0.51, 0.45, 0.86, and 0.48, respectively, and suggesting more or less organic affinity of these oxides (Table 5). The positive correlations of these oxides with the TMC (total maceral content) support the above interpretation. The oxide compositions are also useful to depict the climatic conditions that prevailed during peatland formation (following McLennan et al. 1993). The calculated CIA and CIW indices (Table 1) were correlated with the Universal Continental Crust (UCC) values (following McLennan, 2001). It has been observed that the studied samples have greater values than the UCC values (CIA = 60.11 and CIW = 70.89).

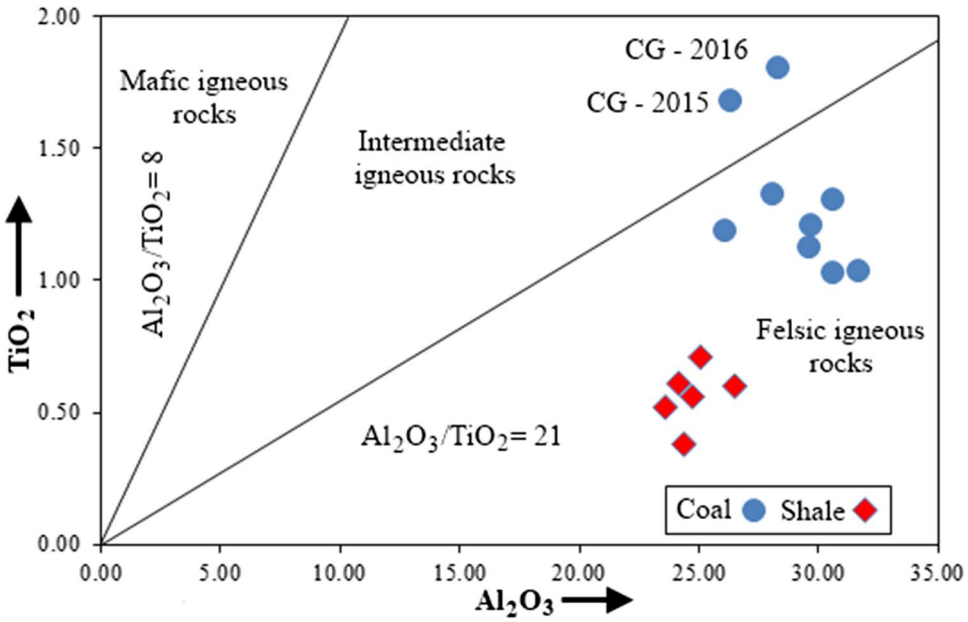

Fig. 3 The plot of TiO_2 vs Al_2O_3 diagram (wt.%) for coal and shale samples of Makum Coalfield, India (Amajor, 1987 and Imchen et al. 2014)

Table 5 Pearson's correlation coefficient for the studied samples

	SiO_2^*	$Al_2O_3^*$	$Fe_2O_3^*$	K_2O^*	CaO^*	MgO^*	TiO_2^*	$P_2O_5^*$	Na_2O^*	SO_3^*	A^d	FC	S^{daf}	TMC
SiO_2^*	1.00													
$Al_2O_3^*$	-0.65	1.00												
$Fe_2O_3^*$	-0.96	0.58	1.00											
K_2O^*	0.48	-0.75	-0.38	1.00										
CaO^*	-0.51	0.17	0.34	-0.52	1.00									
MgO^*	-0.33	0.22	0.21	-0.48	0.68	1.00								
TiO_2^*	-0.83	0.57	0.68	-0.59	0.70	0.46	1.00							
$P_2O_5^*$	0.18	-0.34	-0.26	0.27	0.14	-0.22	-0.07	1.00						
Na_2O^*	-0.82	0.33	0.71	-0.15	0.52	0.14	0.79	0.17	1.00					
SO_3^*	-0.86	0.48	0.91	-0.30	0.23	-0.08	0.59	-0.13	0.70	1.00				
A^d	0.75	-0.82	-0.62	0.84	-0.58	-0.49	-0.85	0.21	-0.52	-0.48	1.00			
FC	-0.72	0.80	0.58	-0.85	0.60	0.48	0.86	-0.19	0.51	0.45	-1.00	1.00		
S^{daf}	0.08	-0.27	0.08	0.63	-0.49	-0.33	-0.33	-0.06	-0.10	0.07	0.43	-0.46	1.00	
TMC	-0.78	0.78	0.64	-0.85	0.66	0.53	0.88	-0.16	0.57	0.51	-0.98	0.98	-0.49	1.00

Explanations: *in molecular proportion; A: ash yield on dry basis (wt. %); *FC:* fixed carbon (wt. %), *S:* sulfur on dry ash free basis (wt. %), *TMC:* total maceral content (vol. %)

This indicates that coal has experienced moderate to strong weathering, whereas very high weathering under warm and humid atmospheric conditions is observed in shales (Nesbitt and Young, 1982; Fig. 4). The high weathering condition experienced by the OM might be due to a warm climate during the Oligocene, and also, the rainfall was sufficiently high under these climatic conditions, which intensified the weathering intensity (Biswas, 1987). This condition is also suitable for the growth of microorganisms and the abundant microbial activity in the source area creates more and more chemical weathering. Furthermore, the CIA and CIW indices are applied to determine the weathering conditions that the sediments have undergone. The ternary diagram of Al_2O_3, ($CaO + Na_2O$), and K_2O exhibits that the coal samples are characterized by intermediate clay composition varying from smectite to kaolinite, whereas shales are plotted close to the illite field due to the presence of a comparatively higher amount of K_2O (Nesbitt and Young, 1982; Fig. 4). The occurrence of such clay minerals in the samples indicates inorganic sediments are primarily sourced from

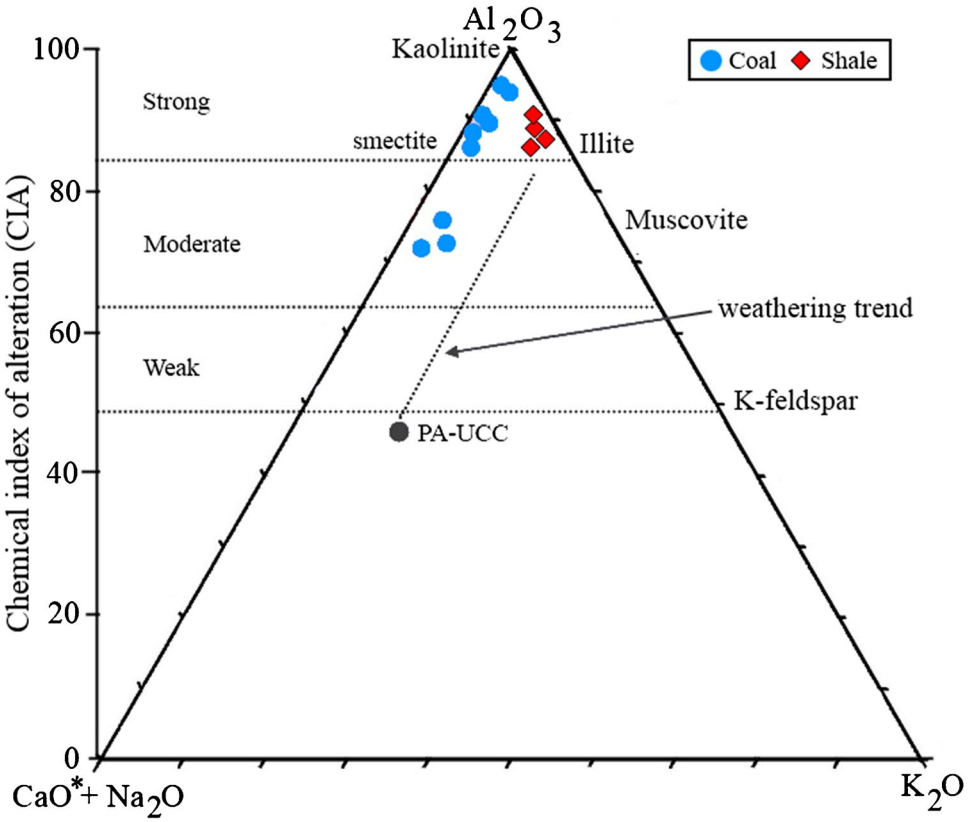

Fig. 4 Al_2O_3, $CaO^* + Na_2O$, K_2O ternary diagram showing CIA (chemical index of alteration) of studied coal and shale samples (Nesbitt and Young, 1982). Post-Archean upper continental crust (PA-UCC) (after Rudnick and Gao, 2004)

mixed felsic rocks, i.e., mostly granodiorite and granite. In contrast, the presence of smectite is indicative of weathering by-products from basic rocks (Grant, 1963 and Patterson, 1971).

The modes of occurrence of the inorganic matters present in the source rock are measureable through use of the X-ray diffractometer. The diffractogram patterns are generally poorly developed in coal, which might be due to coal's large OM compounds and also, they are of low rank, whereas prominent peaks are observed in shales, indicating that these are in crystalline form (Fig. 5). Ward (1991), Hochella et al. (2008), and Li et al. (2010) reported that at low ranks and associated less maturation levels, inorganic minerals occur as poorly crystalline or even as being amorphous. The XRD results reveal that samples are mostly quartz, wollastonite, nepheline, magnetite, spinel, corundum, berlinite, and mullite minerals (Table 2). The presence of the carbonate phase within the samples indicates brackish water to marine environment of deposition. Likewise, the occurrence of quartz and microcline (potassium-rich alkali feldspar) suggests that they were derived from the siliceous and felsic igneous rock, respectively (Ward, 2002). This further indicates that probably granite or granodiorite rocks are the main sources for inorganic matter within the coalfield. The interpretation from the XRD analysis corroborates the XRF analysis in determining the sources of inorganic matter in the peatland. The geochemical plot of MgO/Al_2O_3 and K_2O/Al_2O_3 (Fig. 6; Shehata and Abdou, 2008) shows that most of the coal and shale samples are plotted in the zone of a marine environment, and some shales (CG, 2003; CG, 2014; CG, 2019) are in the zone between non-marine and marine. This indicates that they are largely deposited in an upper delta-plain environment, but there is an indication of periodic marine water incursion during shale formation as directed by the elevated concentration of K_2O and MgO. This might be due to the rise of sea level during the Oligocene epoch. Miller et al. (2005) also reported changes in global sea-level conditions during the Oligocene to early Pliocene mostly due to the growth and decay of the Antarctic ice sheet. Furthermore, several relations such as [(K_2O/Na_2O) vs SiO_2)], [$(MgO + Fe_2O_3)$ and TiO_2], and [$(MgO + Fe_2O_3)$ with (Al_2O_3/SiO_2)] have been observed to provide a framework for understanding the paleotectonic setting of the studied area (Bhatia, 1983; Roser and Korsch, 1986; Xiao et al. 2008; Fig. 7). The discrimination plots suggest that the inorganic or mineral matter present in the coal and shale units was derived from passive-to-active continental margin settings. Mishra and Ghosh (1996) and Singh and Singh (2000) also support this observation and

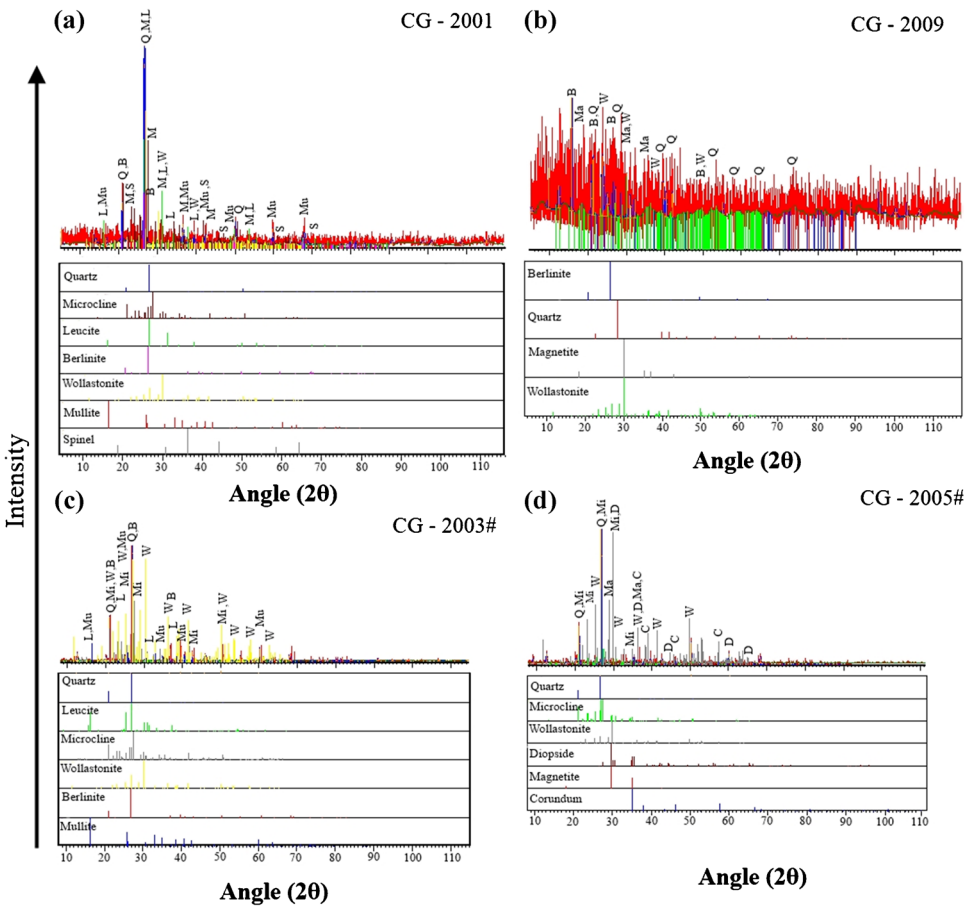

Fig. 5 XRD spectra of coal (**a**, **b**) and shale (**c**, **d**) samples. Explanations: Q: quartz, B: berlinite, W: wollastonite, Mi: microcline, L: lucite, S: spinel, Mu: mullite, Ma: magnetite, C: corundum, D: diopside

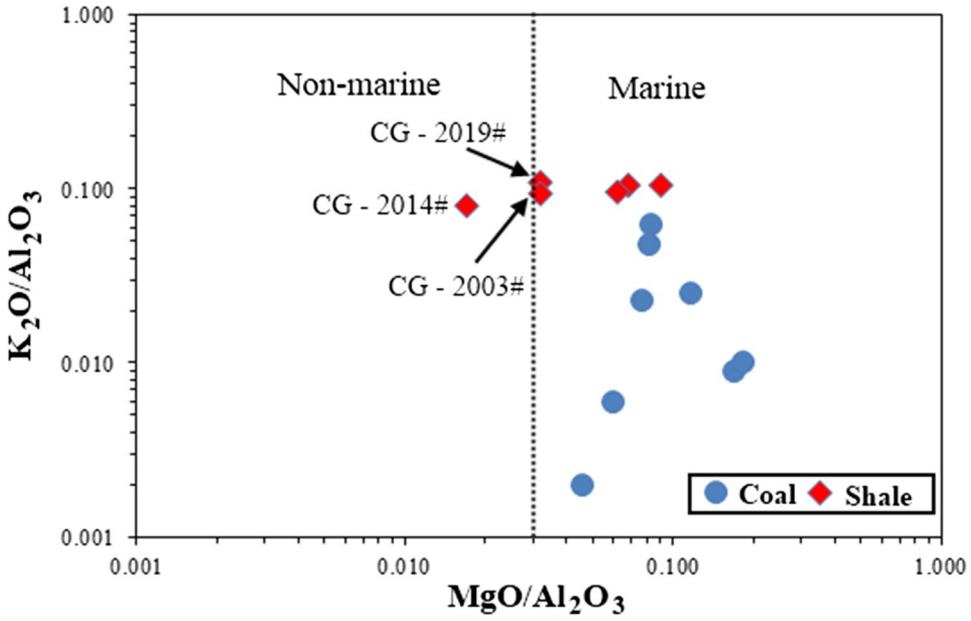

Fig. 6 Depositional environments based on MgO/Al_2O_3 and K_2O/Al_2O_3 (following Roaldest, 1978)

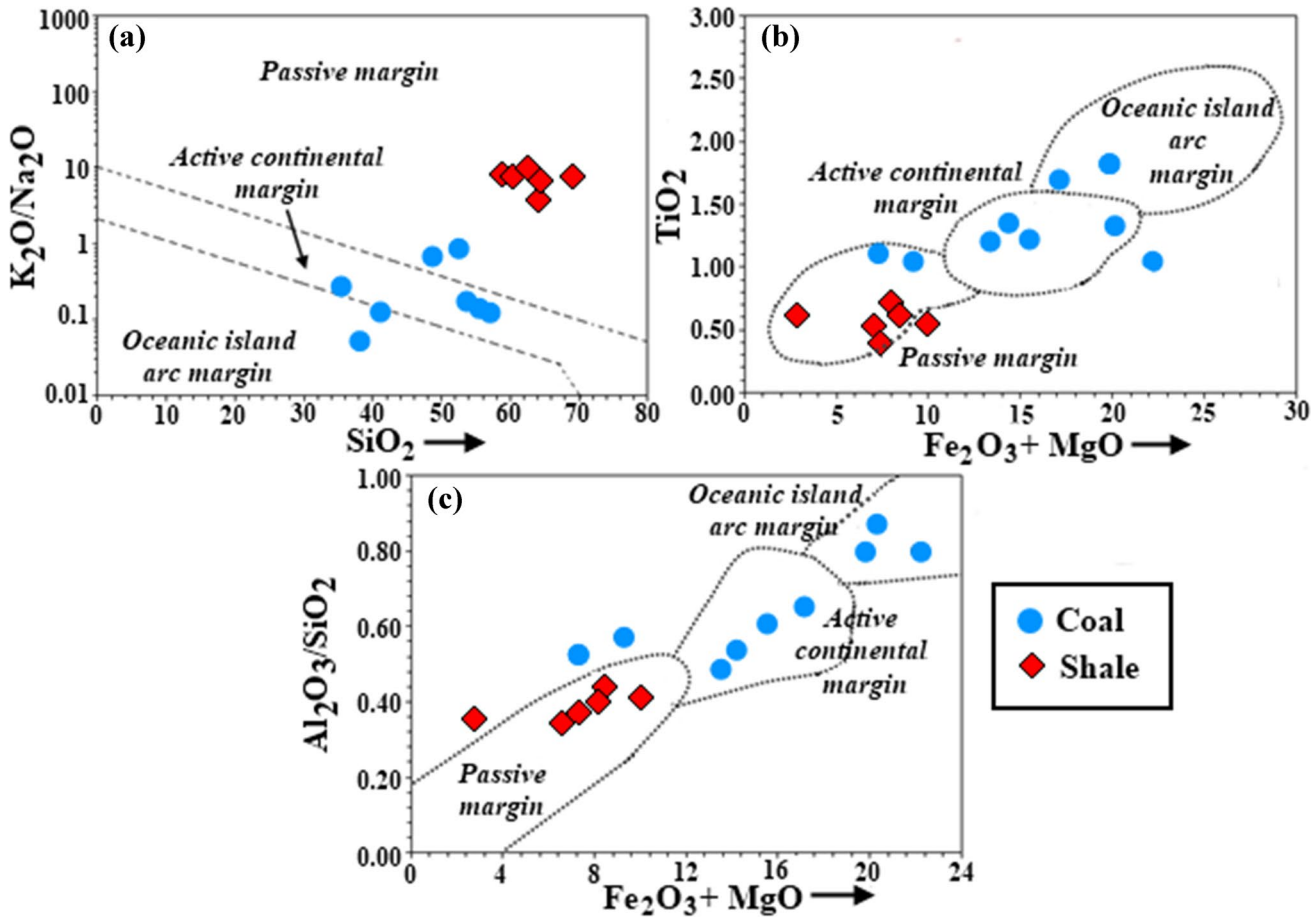

Fig. 7 Discrimination of tectonic settings based on oxide compositions of the coal and shale from Makum Coalfield, India. **a** After Roser and Korsch (1988), **b** and **c** after Bhatia (1983)

have pointed out that the Oligocene Barail Group was deposited in a marine-deltaic-estuarine environment in a passive, continental margin setting. The multiple phase transformation in the environment might due to large-scale changes in tectonic and climatic conditions during the Eocene-to-Oligocene epoch and helps in the evolution of marine and terrestrial biota (Schouten et al. 2007, McInerney and Wing, 2011, and Rudra et al. 2017). Moreover, the salinity of the water during the deposition has been determined from the proposed formula by Yu et al. (2014). The equation is as follows:

$$\text{Salinity} = [\text{MgO}/\text{Al}_2\text{O}_3] \times 100 \quad (3)$$

The salinity value of most samples lies between 1 and 10 and implies transitional depositional conditions, i.e., a delta-plain environment (Veizer and Demovic, 1974; and Jarvis et al. 2001). Some coal samples (i.e., CG, 2001; CG, 2007; and CG, 2009) possessing high salinity values > 10 point towards incursion of marine water during peatland formation. The positive correlation of the salinity value with the MgO having $r^2 = 0.99$ also supports the aforementioned observation.

OM depositional conditions

The combination of organic petrography and palynofacies analysis both provide valuable information about the depositional environment and paleoclimatic conditions of the coal and shale forming peatland formations (Tissot and Welte, 1978; Stach et al. 1982; Mukhopadhyay, 1986; Kalkreuth et al. 1991; Diessel, 1992; Tyson, 1995; Batten, 1996a, b; Erik, 2011; Mendonça Filho et al. 2011, 2012). Understanding the accumulation of the organic matters (OM) and their depositional environment is also very essential to improve hydrocarbon exploration potential of the Tikak Parbat Formation (Oligocene) in Makum area.

Petrographic characteristics

The maceral compositions through petrographic study suggest that the coal and shale in the Tikak Parbat Formation are largely vitrinite (together ranging from 5.58 to 66.86 vol. %) with a considerable amount of liptinite (together varies from 7.26 to 34.46 vol. %) and a small quantity of inertinite macerals (Table 3). The vertical maceral distribution shows that vitrinite content gradually decreases from the 60 feet top coal seam to the 20 feet coal seam and it progressively increases in the 8 feet coal seam (Fig. 8). The higher vitrinite content in the bottom and top of the formation indicates periodic changes in water-covered reducing environmental conditions due to the fluctuation of water level in the peatland. The liptinite macerals also increase progressively from bottom to top. But there is no such substantial variation of inertinite macerals throughout the formation. The presence of a significant amount of vitrinite (Fig. 9) designates that coal/shale forming peat is made up of megathermal plants, and herbaceous vegetation matter, deposited in waterlogged or moist swamp forest conditions (Flores, 2002; Petersen et al. 2009; Erik, 2011). Likewise, terrestrial liptinites (Fig. 9) such as resinite, sporinite, cutinite, and suberinite in the samples also indicate similar peat depositional environments. Bituminite occurs in both amorphous and lamellar form and is observed in all the samples, and implies those might originate from biodegraded higher plants. The occurrence of a small amount of inertinite macerals also is suggestive of low oxidation conditions in the peatmire and also of low occurrences of naturally caused forest fires (Fig. 9). The presence of funginite indicates degraded OM in the samples (Hower et al. 2010, 2011; and O'Keefe and Hower, 2011). To acquire additional information on their depositional conditions within the peatland, an organofacies diagram was been prepared, based on maceral assemblages (modified after Mukhopadhyay, 1986 and Kalkreuth et al. 1991). Study of the ternary plot suggests that the coal and shale forming peat has well-preserved tissues and was deposited under mildly oxic-to-anoxic forest-to-limnic swamp conditions (Fig. 10). This also confirms that the groundwater table in the mire was high, which prevented oxidation of OM. This interpretation is supported by the presence of a trace amount of oxidizing macerals within the samples analyzed. The plot also shows that all the coals are mapped on the left side, which exhibits megathermal plants, ferns, pteridophytes spores, and pollen might be the major component of the vegetation. Likewise, shales plot on the right side of the diagram, which further points towards herbaceous plant species (reed, marsh, helophytes, etc.), were the dominant contributing component of vegetation rather than woody plants. These data in Fig. 10 are furthermore suggestive of terrestrial land plants being dominant contributors for the OM source in the Oligocene sediments. Kumar et al. (2012) also reported that land plants such as palms, mangroves, different types of ferns, angiosperms, and conifers are contributing to the formation of Oligocene coal and shale in the Makum Coalfield. In addition to this, various minerals are also indicative of the peat depositional environment. The coal samples having relatively less mineral material in comparison to shales are exhibited in Table 3. The identified minerals under petrographic analysis are mostly quartz, clay, pyrite, calcite, and siderite. Among them, quartz and clay minerals are mostly associated with the macerals and occur as granules and/or lump shaped inclusions, whereas pyrite occurs in variable array of forms like framboidal and disseminated (Fig. 9 f–h). Pyrite also occurs in the veins and cracks of OM and their concentration is observed to be higher in shale than in coal. The occurrence of pyrite

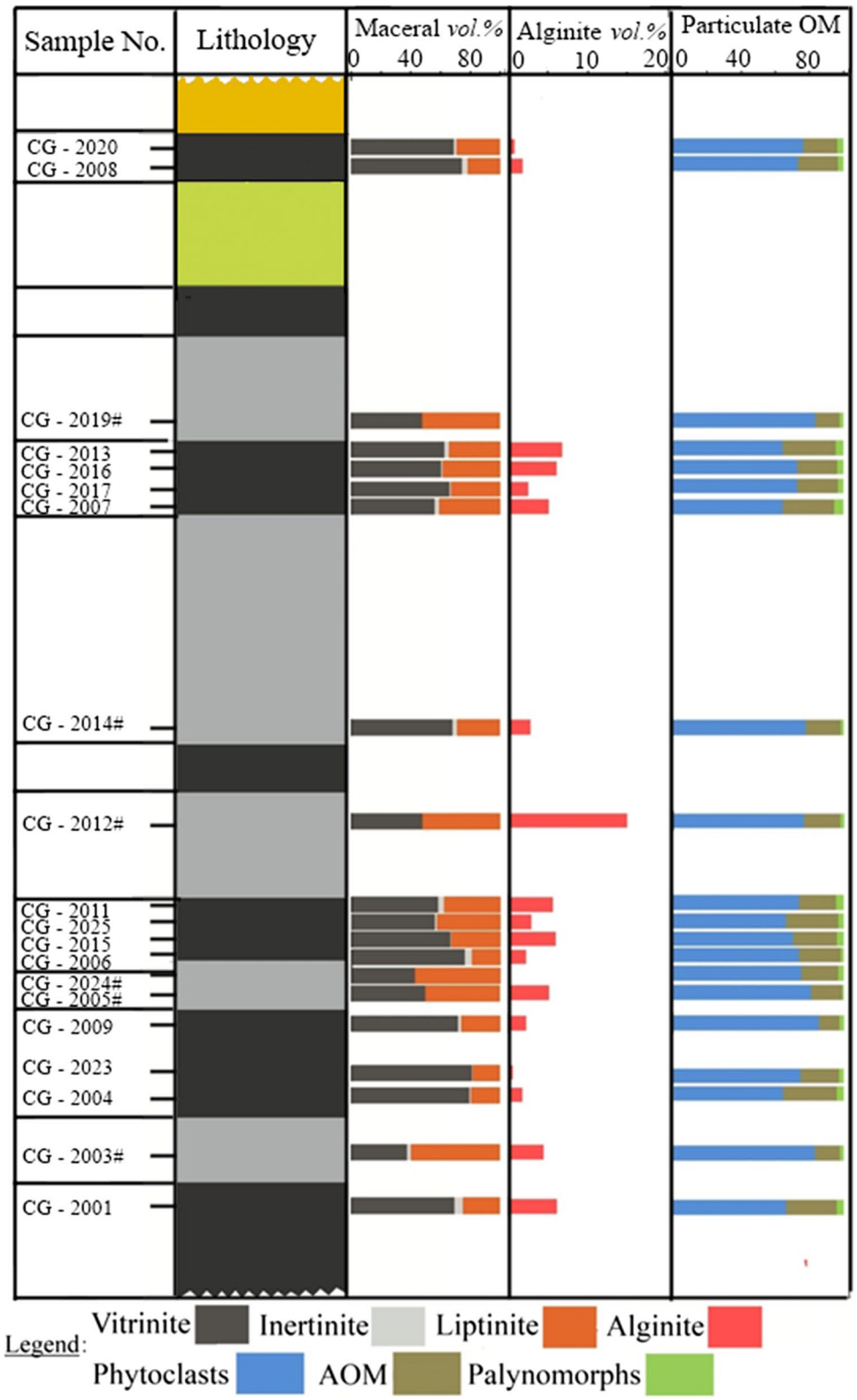

Fig. 8 The organic matter variations across the seams of Tikak Parbat Formation, Makum Coalfield, India. Explanation: AOM = amorphous organic matter

crystals in the samples indicates syngenetic or early diagenetic origin. The presence of framboidal-type pyrite points towards the existence of marine water during the peatland formation and its influence is more pronounced during sedimentation associated with the shale units, probably due to the rise of sea level (Kuder et al. 1998). Carbonate minerals such as calcite and siderite are also recorded and occur sporadically in the studied samples.

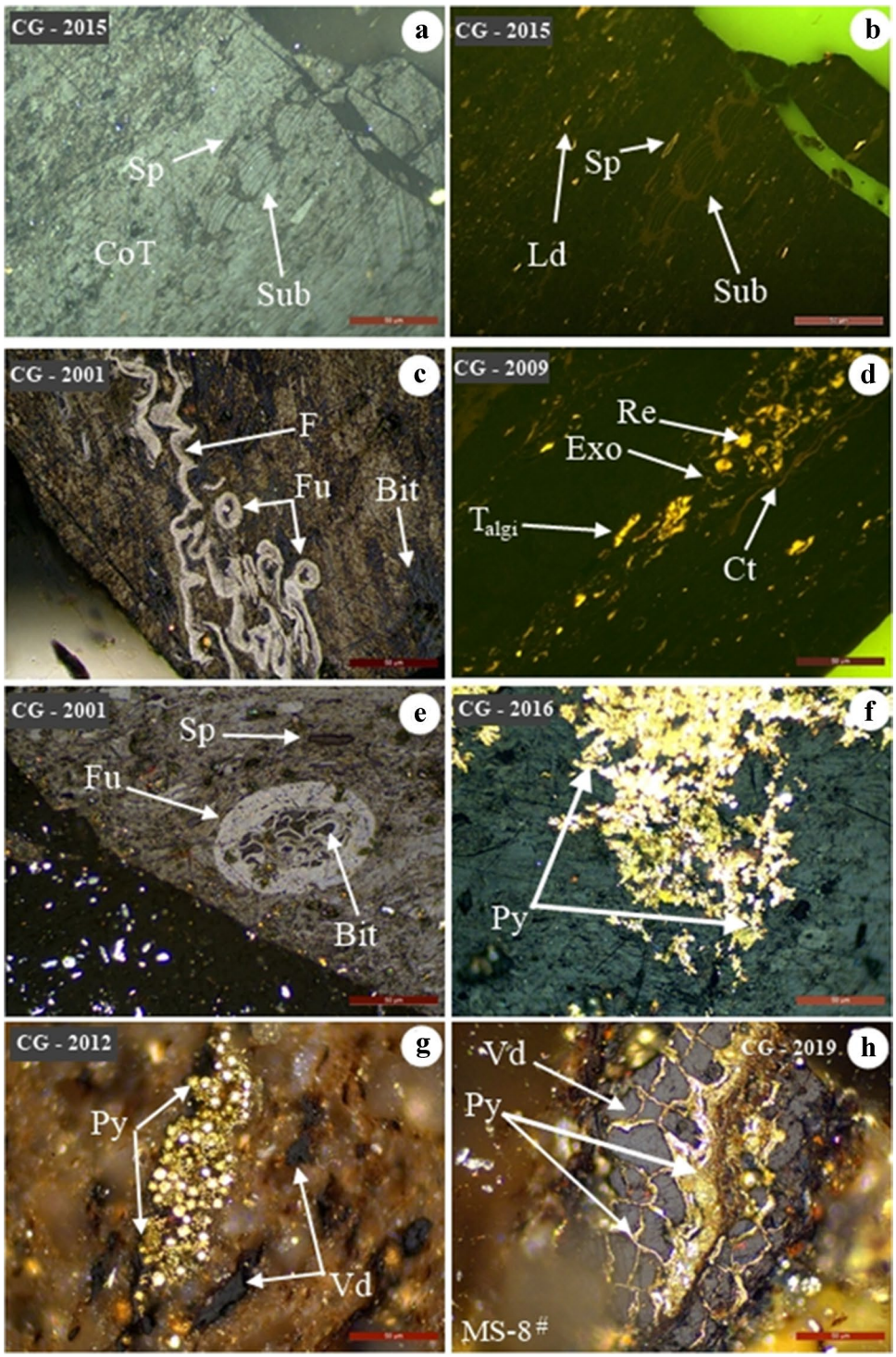

Fig. 9 Photomicrographic characteristics of Makum coal and shale samples: (**a**) collotelinite (CoT) matrix hosting sporinite (Sp), suberinite (Sub), and liptodetrinites (Ld); (**b**) similar photographs as "a," taken under fluorescent light; (**c**) collotelinite (CoT) matrix encompasses bituminite (Bit), funginite (Fu), and fusinite (F), bituminite is also preserved within the cavity of funginite; (**d**) assemblages of globular shaped resinite (Re), cutinite (Ct), exsudatinite (Exo), and telalginite (T_{algi}), taken under fluorescent light; (**e**) collotelinite (CoT) matrix hosting funginite (Fu), resinite (Re), and cavity of funginite is filled with bituminite (Bit); (**f**) disseminated pyrite (Py) within coal samples; (**g**) agglomeration of framboidal pyrite (Py) and fragments of vitrodetrinite (Vd) within shale; (**h**) cracks filled with pyrite (Py)

Furthermore, to more elucidate the condition of organic matter deposition within the peatland, the authors have studied the sulfur content of the samples through ultimate analysis. The result shows a wide range of sulfur (S^{daf}) in coal and shale ranges from 1.27 to 9.45 wt. % (avg. 4.27 wt. %) and 1.83 to 19.03 wt. % (avg. 10.03 wt. %), respectively. This suggests the overlapping of non-marine to marine conditions within the peatland (Sykes et al. 2014). Chou (2012) also pointed out the low sulfur content represents the freshwater environment, whereas the marine environment is exhibited by a large amount of sulfur. The higher amount of sulfur (avg. 6.70 wt. %) in the samples is likely due to the penetration of seawater into the peats as a result of basin-floor subsidence. Several scientists (Querol et al.

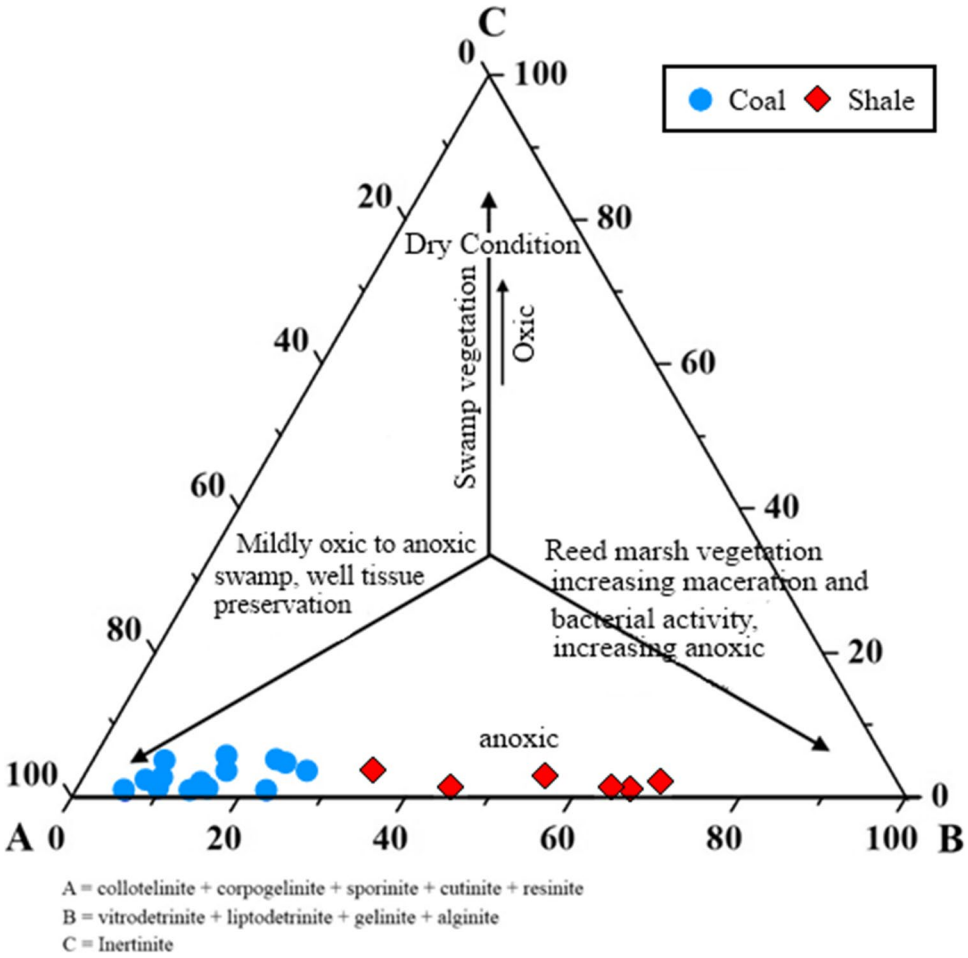

Fig. 10 Ternary diagram of peat-forming environments from maceral compositions of the studied samples from Makum Coalfield, India (after Mukhopadhyay, 1986)

1996; Kuder et al. 1998; Gürdal, 2008) have also reported about the sulfur enrichment during the peat formation of different coal basins.

Palynofacies characteristics

Palynofacies are also an important and reliable tool to typify OM, their paleodepositional conditions, and hydrocarbon generation. Investigation of the palynofacies record suggests that the recovered OM are dominantly phytoclasts, with some amount of amorphous organic matter (AOM) and palynomorphs (following Tyson, 1995; Batten, 1996a, b; Mendonça Filho et al. 2011, 2012; Fig. 11). Among the phytoclasts group, the concentration of non-opaque phytoclasts is higher than that of opaque phytoclasts, indicating the low intensity of natural forest fires in the peatland. The biodegraded OM under non-opaque phytoclasts are marked by non-cellular structure (Fig. 11), but in some portion, the mild cellular structure has also been observed, mostly originating from plant cuticles (Batten, 1996a, b). The amount of wood, cuticles, and biodegraded matter in both coal and shale implies that they might come from plants growing closer to the depositional area (Table 4). The AOM can originate from bacterial/fungal degradable plant material or from excremental parts of zooplankton (Tyson, 1995), whereas resins are mostly from higher land plants. The more or less homogenous distribution of resins throughout the formation suggests that wood vegetation is more pronounced than is aquatic plant matter (Table 4). Likewise, palynomorphs are the least abundant and are characterized by sporomorphs (spore/pollen) and fungal filaments (Fig. 11). Table 4 shows a uniform distribution of spore and pollen grains, and this suggests that tree ferns are most abundant during the Oligocene epoch, and these contribute significantly to peat formation. The abundance of biodegraded OM, AOM, and resins from the bottom to the top of the formation suggests they were deposited under low oxygen or anoxic environmental conditions.

In addition to this, a ternary diagram of phytoclasts, AOM, and palynomorphs has been plotted and shows that the studied coal and shale are all plotted in field-II, which also exhibits marginal dysoxic-or-anoxic depositional conditions (Demaison and Moore, 1980; Tyson, 1995; Fig. 12). Kumar et al. (2012) also reported that Oligocene coal and

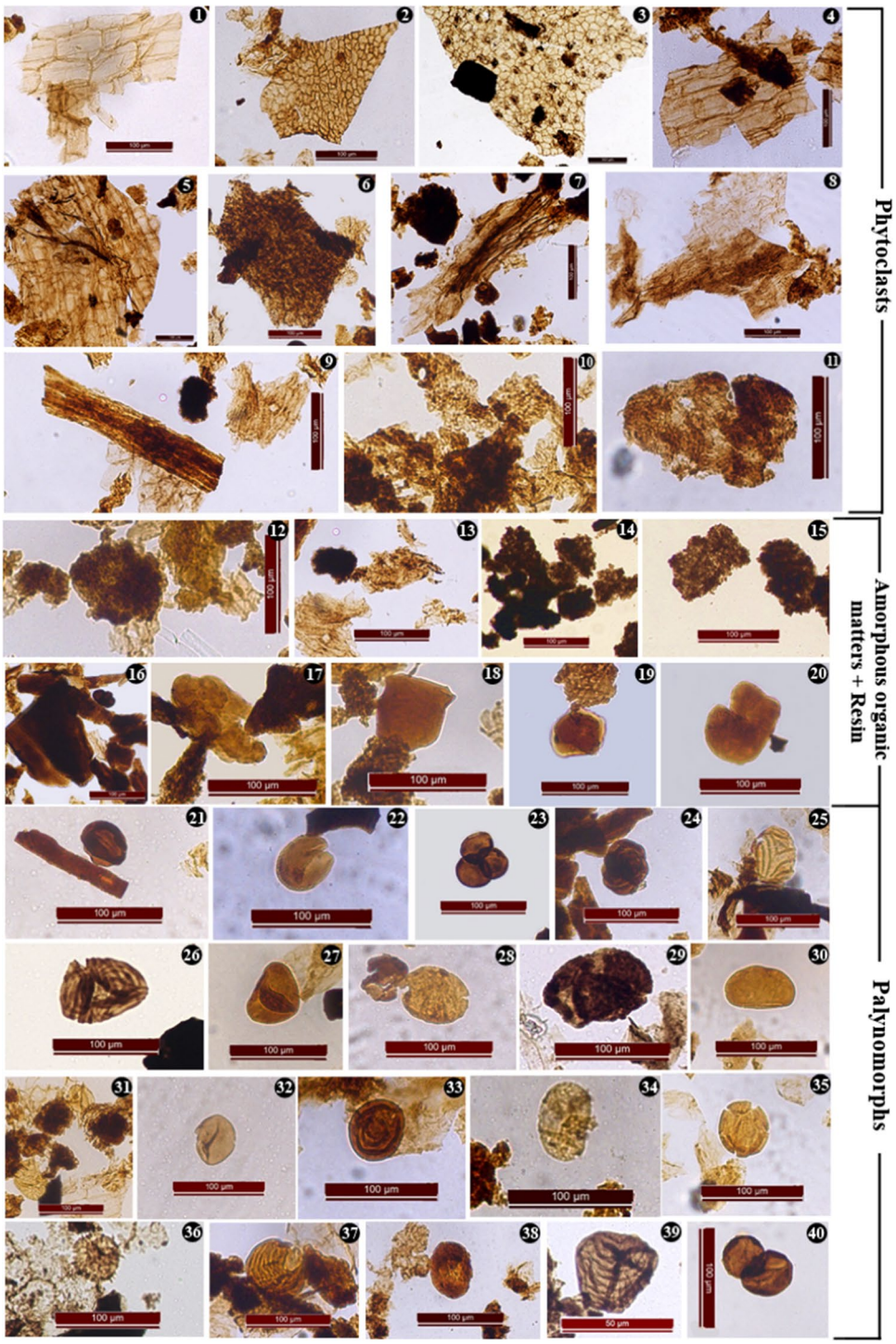

Fig. 11 Microphotographs of the phytoclasts (1–11), amorphous organic matter (AOM) + resin (12–20), and palynomorphs (21–40) groups of OM observed in the studied samples of the Makum Coalfield, India. Note: 1–3 = cuticle; b: 4–11 = biodegraded; 3, 5, 7 = black debris; 12–15 = amorphous organic matter; 16–20 = resin; 21–40 = sporomorphs (spores and pollens)

shale are made up of megathermal forests and mostly deposited under anaerobic to dysaerobic freshwater environments. This type of environment mostly occurred in the coastal areas and was formed by fluvial, wave, or tidal influenced basinal processes. Continued sedimentation partially by fluvial, marine, and organic sedimentation fills the low-lying areas and subsequently converts them into coastal swamps. A variety of plants (mostly wood, grasses, and reeds) were the species that thrived and formed dense vegetation into the swamps and such biomasses gradually were transformed into fossil fuels (Diessel, 1992). Algae are the main contributors to the accumulating organic mud which may be covered and laterally replaced by peat when paludal conditions succeed the lagoons (Stach et al. 1982; Diessel, 1992). The coastal low-lying areas are mostly separated from the sea either by a barrier beach or by a mangrove belt (Diessel,

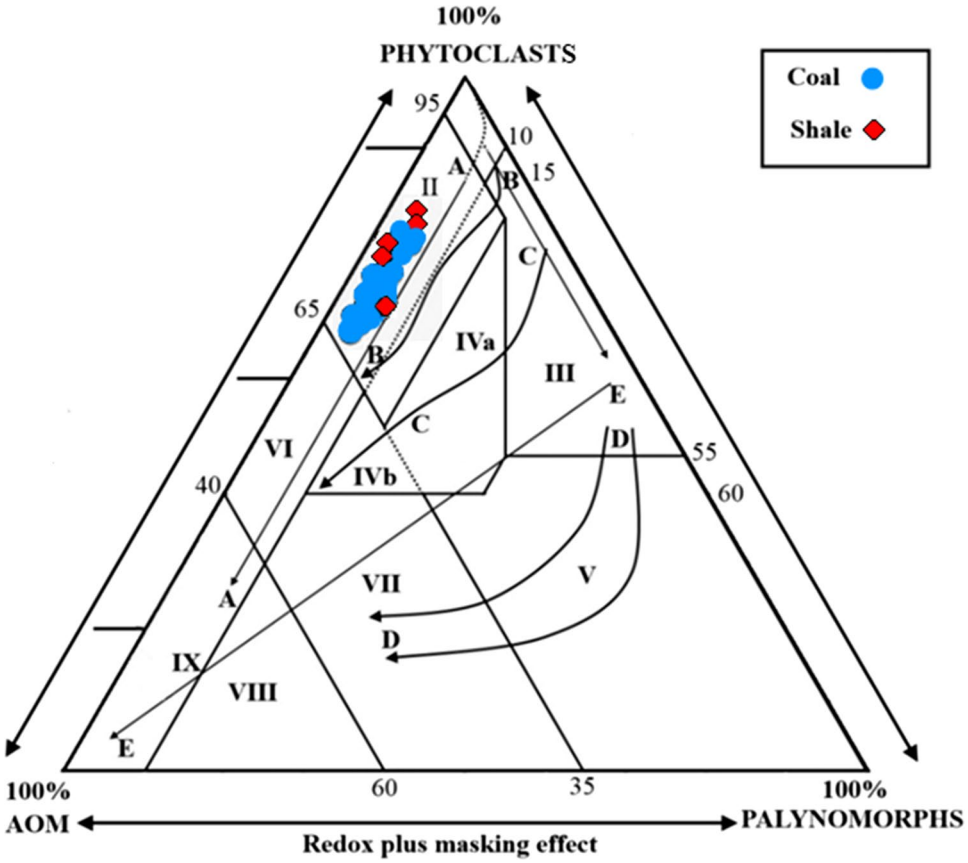

Fig. 12 Ternary APP diagram (following Tyson, 1995) showing depositional environment condition and kerogen type. Explanation: AOM: amorphous organic matter; I to IX: name of the fields, which indicates possible depositional environment (note: I = highly proximal shelf basin; II = marginal dysoxic-anoxic basin; III = heterolithic oxic shelf; IV = shelf to basin transition; V = mud-dominated oxic shelf; VI = proximal suboxic-anoxic shelf; VII = distal dysoxic-anoxic shelf; VIII = distal dysoxic-oxic shelf; IX = distal suboxic-anoxic basin)

1992). Sykes et al. (2014) reported that the coaly source rocks which are mostly found in the coastal plain settings are known to be oil-prone. For example, in Australia and Indonesia, the coastal sediments are the most important source rocks for natural gas and oil (Thomas, 1982; Durand and Paratte, 1983; Thompson et al. 1985; Shanmugam, 1985; Khavari Khorasani, 1987; Horsfield et al. 1988; Hvoslef et al. 1988; Rice et al. 1989). The palynofacies assemblages suggest that both coal and shale having mixed kerogen type (type III + II + I) are reflective of gas and oil-prone source rocks (following Tyson, 1995). The obtained reflectance values for the coal and shale indicate they are in the field of immature-to-early mature, but some of them are near to the oil birth line (Espitalié et al. 1985; Peters and Cassa, 1994). This suggests that the onset of hydrocarbon formation has been generated from the source rock and with increasing maturity, they are capable of producing mixed thermogenic gas and some condensate oil. Additional support of this observation is a ternary plot of the vitrinite, inertinite, and liptinite (VIL plot) that has been prepared exhibiting maceral assemblages (Tissot and Welte, 1978; Shalaby et al. 2019; Singh and Kumar, 2017). A previous study shows that the amount of liptinite is very much essential in order to generate liquid hydrocarbons (oil), but there are many different views. Hunt (1991) pointed out that 15 to 20 vol. % of liptinites are necessary to generate oil. Similarly, Snowdon (1991) suggested that as little as 10 vol. % H-rich macerals are essential for oil generation. Mukhopadhyay et al. (1991) considered 20 to 25% liptinite to generate > 10 wt. % pyrolysate. In this study, we have considered both liptinite and vitrinite macerals, as they are known to produce liquid and gaseous hydrocarbons, respectively. On the basis of their amount (i.e., liptinite ≥ 25 vol. % and vitrinite ≥ 55 vol. %), the VIL plot has been slightly modified and accordingly, the "mixed oil and gas" zone has been split into "oil dominating and minor gas" (i.e., uppermost zone) and "gas dominating and minor oil" (i.e., lowermost zone). Most of the coal samples are plotted below the zone which indicates dominance of gas generation, and shales are plotted slightly above the zone exhibiting more oil generation (Fig. 13). This also substantiates the above observation from the palynofacies study.

Conclusions

The multifaceted study of mineralogy, organic petrography, and palynofacies assemblages reveals that the coal and shale of the Makum Coalfield were deposited under a mildly oxic-to-anoxic deltaic forest to limnic swamp condition. Megathermal trees, ferns, pteridophytes spores, and pollens might

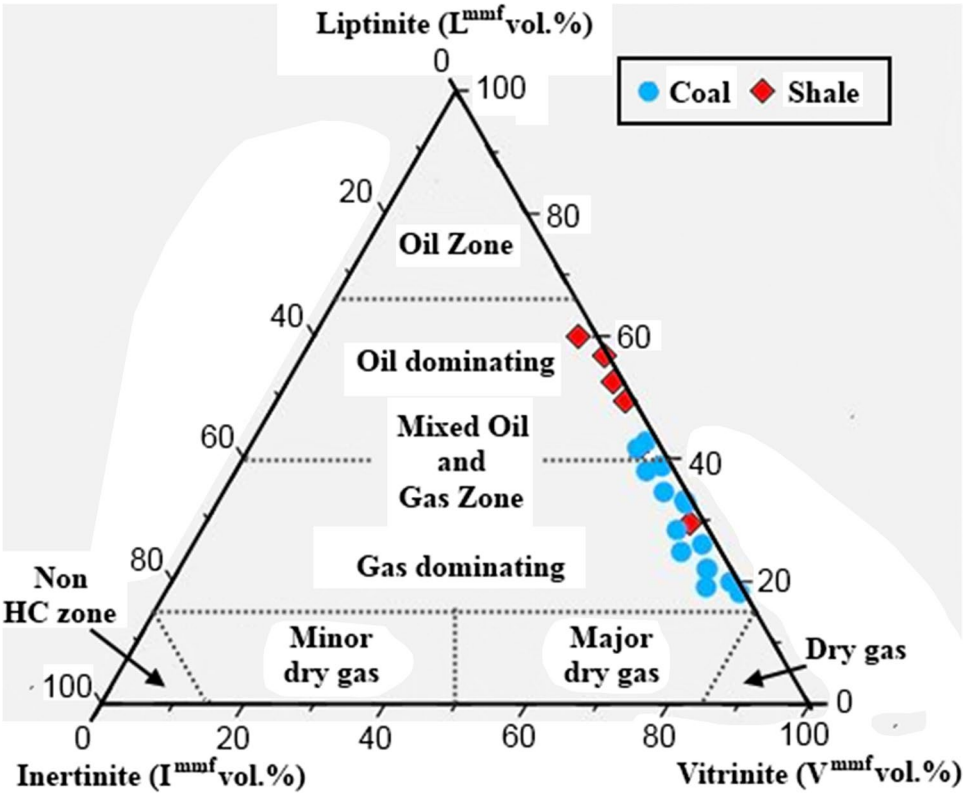

Fig. 13 Ternary diagram based on maceral assemblage for the coal and shale from the Makum Coalfield, India (slightly modified after Tissot and Welte, 1978)

be the major component of the vegetation for coal formation, whereas herbaceous plant species, such as reed, marsh, helophytes, etc., made the shale beds. The dependence of higher plant organic matter (OM) on floral precursors is mainly controlled by the combination of depositional conditions, i.e., water level, temperature, salinity, etc. The periodic marine water incursion during shale formation in the basin might be due to the sea-level rise and further indicates changes in global sea-level conditions during the Oligocene to early Pliocene epoch. The inorganic matter is mostly composed of quartz, feldspar, calcite, magnetite, spinel, corundum, berlinite, mullite, pyrite, and some clay minerals. The occurrences of these minerals are representative of being derived from a passive-to-active continental margin setting. In addition, deposition of OM under high water level in the peat and moderate-to-strong weathering of inorganic matter also reveals the change in tectonic and climatic conditions during the Oligocene epoch. Depositional conditions were suitable for the accumulation of diversified plant species, and with sufficient basinal thermal maturity, both coal and shale might be recognizable as economically important thermogenic gas and oil, respectively.

Acknowledgements The authors are thankful to Prof. Abdullah M. Al-Amri (Editor-in-Chief) and anonymous learned reviewers for critical evaluation and valuable suggestions to improve the quality of the manuscript. Authors are grateful to the Officers of the North-East Coalfields Limited, Assam, India, for their valuable help in collecting samples. We appreciate the guidance and support from Dr. Bhagwan D. Singh, Emeritus Scientist of BSIP, Lucknow, India, for carrying out the palynofacies analysis. The authors would like to acknowledge Mr. Amal Kishore Prasad, Research and Development Centre for Iron and Steel (RDCIS), Ranchi, India, for his valuable support in evaluating the X-ray fluorescence (XRF) analysis results. The authors would like to acknowledge the Technical Education Quality Improvement Programme of Government of India (TEQIP-III) of IIT (ISM) Dhanbad for financial assistance to conduct X-ray diffraction (XRD) analysis from the National Centre for Earth Science Studies (NCESS), India. The modern facilities in the Dept. of Applied Geology, IIT (ISM) Dhanbad, were funded by the Department of Science and Technology (DST) within the Ministry of Science and Technology, Government of India, under the scheme of "DST-FIST Level II" [no. SR/FST/ES II 014/2012(C)].

Data availability Not applicable.

Code availability Not applicable.

Declarations

Conflict of interest The authors declare no competing interests.

References

Ahmed M (1989) Characters of Tertiary coal of Makum coalfield, Assam, northeast India, and its utilization prospects and constraints. 28th Int. Geol. Congr. Washington, DC, Abstr 3:21–22

Ahmed M (1996) Petrology of Oligocene coal, Makum coalfield, Assam. Northeast India Int J Coal Geol 30:319–325. https://doi.org/10.1016/0166-5162(95)00051-8

Alkande SO, Hoffknecht A, Erdtmann BD (1992) Rank and petrographic composition of selected Upper Cretaceous and Tertiary coals of southern Nigeria. Int J Coal Geol 20:209–224. https://doi.org/10.1016/0166-5162(92)90014-N

Amajor LC (1987) Major and trace elements geochemistry of Albian and Turonian shales from the Southern Benue trough. Nigeria J Afr Earth Sci 6:633–641. https://doi.org/10.1016/0899-5362(87)90002-9

ASTM, 1994. Standard test method for microscopical determination of the reflectance of vitrinite in a polished specimen of coal. D2798–96. Annual Book of American Society for Testing and Materials Standards: Gaseous Fuels: Coal and Coke; Sec.5 5.05 279–283.

Batten, D.J., 1996a. Palynofacies and palaeoenvironmental interpretation. In: Jansonius, J., Mc Gregor, D.C. (Eds.), Palynology: Principles and Applications. 3. AASP, 1011–1064.

Batten, D.J., 1996b. Palynofacies and petroleum potential. In: Jansonius, J., Mc Gregor, D.C. (Eds.), Palynology, Principles and Applications. vol. 3. AASP, 1065–1084.

Batten DJ (1999) Palynofacies analysis. In: Jones TP, Rowe NP (eds) Fossil Plants and Spores. Modern Techniques. Geol. Soc, London, pp 194–198

Batten DJ, Stead DT (2005) Palynofacies analysis and its stratigraphic application. In: Koutsoukos EAM (ed) Applied Stratigraphy. Springer, Dordrecht, Netherlands, pp 203–226

Bhandari LL, Fuloria R, Sastry VV (1973) Stratigraphy of Assam Valley, India. Bull American Association of Petroleum Geologists 57(4):642–650. https://doi.org/10.1306/819A4310-16C5-11D7-8645000102C1865D

Bhatia MR (1983) Plate tectonics and geochemical composition of sandstones. J Geol 91(4):611–626. https://doi.org/10.1086/628815

Biswas S (2021) Petrographic and geochemical controls on coal and shale for hydrocarbon generation from Makum and Barjora Basins of India: experimental modeling. Ph.D. Thesis. Indian Institute of Technology (Indian School of Mines), Dhanbad, India. (unpublished).

Biswas S, Varma AK, Kumar M, Mani D, Saxena VK, Mishra V (2020) Influence of geochemical, organo-petrographical and palynofacies assemblages on hydrocarbon generation: a study from upper Oligocene coal and shale of the Makum Coal Basin, Assam. India Mar Pet Geol 114:104206. https://doi.org/10.1016/j.marpetgeo.2019.104206

Biswas SK (1987) Regional tectonic framework, structure and evolution of the western margin basins of India. Tectonophysics 135:307–327. https://doi.org/10.1016/0040-1951(87)90115-6

Bock B, McLennan SM, Hanson GN (1998) Geochemistry and provenance of the Middle Ordovician Austin Glen Member (Normanskill Formation) and the Taconian orogeny in New England. Sedimentology 45:635–655. https://doi.org/10.1046/j.1365-3091.1998.00168.x

Carvalho MA, Mendonça Filho JG, Menezes TR (2006) Paleoenvironmental reconstruction based on palynofacies analysis of the Aptian-Albian succession of the Sergipe Basin. North Eastern Brazil Marine Micropaleontol 59:56–81

Chandra D, Ghose S, Chaudhuri SG (1984) Abnormalities in the chemical properties of Tertiary coals of Upper Assam and Arunachal Pradesh. Fuel 63:1318–1328

Chi Q, Yan M (2007) Handbook of Elemental Abundance for Applied Geochemistry. Geological Publishing House, Beijing, p 148

Chou CL (2012) Sulfur in coals: a review of geochemistry and origins. Int J Coal Geol 100:1–13

Condie KC (1993) Chemical composition and evolution of the upper continental crust: contrasting results from surface samples and shales. Chem Geol 104:1–37

Crosdale PJ (1993) Coal maceral ratios as indicators of environment of deposition: do they work for ombrogenous mires? An example from the Miocene of New Zealand. Org Geochem 20:797–809

Dai S, Bechtel A, Eble CF, Flores RM, French D, Graham IT, Hood MM, Hower JC, Korasidis VA, Moore TA, Puettmann W (2020) Recognition of peat depositional environments in coal: a review. Int J Coal Geol 219:103383

Dai S, Graham IT, Ward CR (2016) A review of anomalous rare earth elements and yttrium in coal. Int J Coal Geol 159:82–95

Dai S, Ren D, Tang Y, Yue M, Hao L (2005) Concentration and distribution of elements in Late Permian coals from western Guizhou Province, China. Int J Coal Geol 61:119–137

Dehmer J (1993) Petrology and organic geochemistry of peat samples from a raised bog in Kalimantan (Borneo). Org Geochem 20:349–362

Demaison GJ, Moore GT (1980) Anoxic environments and oil source bed genesis. Am Asso Petrol Geol Bull 64(8):1179–1209

Dickinson WR, Beard LS, Brakenridge GR, Erjavec JL, Ferguson RC, Inman KF, Knepp RA, Lindberg FA, Ryberg PT (1983) Provenance of North American Phanerozoic sandstones in relation to tectonic setting. Geol Soc Am Bull 94:222–235

Diessel CFK (1992) Coal-bearing Depositional Systems. Springer-Verlag, Berlin, p 721

Durand B, Paratte M (1983) Oil potential of coals: a geochemical approach. In: Brooks J (ed) Petroleum Geochemistry and Exploration of Europe. Blackwell, Oxford, pp 255–265

Erik NY (2011) Hydrocarbon generation potential and Miocene-Pliocene palaeoenvironment of the Kangal Basin (Central Anatolia, Turkey). J Asian Earth Sci 42:1146–1162

Espitalié J, Deroo G, Marquis F (1985) La pyrolyse Rock-Eval etses applications (part I). Rev Inst Fr Pétrol 40:563–579

Evans P (1932) Explanatory notes to accompany a table showing the Tertiary succession in Assam. Trans Miner Geol Met Inst Ind 27:168–248

Flores D (2002) Organic facies and depositional palaeoenvironment of lignites from Rio Major Basin (Portugal). Int J Coal Geol 48:181–195

Francis, W., 1961. Coal, Its Formation and Composition. Edward Arnold, London, 806

Gogoi, K., Dutta, M. and Das, P., 2008. Source rock potential for hydrocarbon generation of Makum coals, Upper Assam, India. Current Science, 95 (2), 233–239. http://www.jstor.org/stable/24103052

Goswami DND (1985) Macerals and low temperature tar of the Tertiary coals of Assam. Meghalaya and Nagaland Geosci J 6(1):95–102

Grant WH (1963) Weathering of Stone Mountain granite. In: Ingersol E (ed) Clays and Clay Minerals. Pergamon, Oxford, United Kingdom, pp 65–73

GSI (Geological Survey of India), 2009. Geology and mineral resources of Assam. Miscellaneous Publication No. 30, Part IV 2.

Gürdal G (2008) Geochemistry of trace elements in Çan coal (Miocene), Çanakkale. Turkey Int J Coal Geol 74(1):28–40

Handique GK, Bharali BT (1981) Temperature distribution and its relation to hydrocarbon accumulation in upper Assam Valley. India Bull Am Assoc Pet Geol 65:1633–1641

Harnois L (1988) The CIW index: a new chemical index of weathering. Sediment Geol 55:319–322

Hayashi KI, Fujisawa H, Holland HD, Ohmoto H (1997) Geochemistry of ~1.9 Ga sedimentary rocks from northeastern Labrador. Canada Geochim Cosmochim Acta 61:4115–4137

Hochella MF, Lower SK, Maurice PA (2008) Nanominerals, mineral nanoparticles, and Earth systems. Science 319:1631–1635

Horsfield B, Yordy KL, Crelling JC (1988) Determining the petroleum-generating potential of coal using organic geochemistry and organic petrology. Org Geochem 13:121–130

Hower JC, O'Keefe JMK, Eble CF, Raymond A, Valentim B, Volk TJ, Richardson AR, Satterwhite AB, Hatch RS, Stucker JD, Watt MA (2011) Notes on the origin of inertinite macerals in coal: evidence for fungal and arthropod transformations of degraded macerals. Int J Coal Geol 86:231–240

Hower JC, O'Keefe JMK, Volk TJ, Watt MA (2010) Funginiteeresinite associations in coal. Int J Coal Geol 83:64–72

Hunt JM (1991) Generation of gas and oil from coal and other terrestrial organic matter. Org Geochem 17:673–680

Hvoslef S, Larter SR, Leythaeuser D (1988) Aspects of generation and migration of hydrocarbons from coal-bearing strata of the Hitra formation, Haltenbanken area, offshore Norway. Org Geochem 13:525–536

IBM, 2019. Coal and Lignite. In: Indian Minerals Yearbook 2018 (Part- III : Mineral Reviews). Ministry of Mines, Nagpur, Maharashtra, India 7 4. http://ibm.nic.in/writereaddata/files/07102019170220COAL_AR_2018.pdf

ICCP (1998) The new vitrinite classification (ICCP system 1994). Fuel 77:349–358

ICCP (2001) The new inertinite classification (ICCP System 1994), International Committee for Coal and Organic Petrology. Fuel 80:459–471

ICDD, 2011. International Center for Diffraction Data. http://www.icdd.com [Accessed 20 March 2011].

Imchen W, Thong GT, Pongen T (2014) Provenance, tectonic setting and age of the sediments of the Upper Disang Formation in the Phek District. Nagaland J Asia Earth Sci 88:11–27

ISO, 2009a. Methods for the petrographic analysis of bituminous coal and anthracite— part 2: methods of preparing coal samples. International Organization for Standardization, ISO, Geneva (8).

ISO, 2009b. Methods for the petrographic analysis of bituminous coal and anthracite— part 3: methods of determining maceral group composition. International Organization for Standardization, ISO, Geneva (4).

ISO, 2009c. Methods for the petrographic analysis of bituminous coal and anthracite— part 5: methods of determining microscopically the reflectance of vitrinite. International Organization for Standardization, ISO, Geneva (11 pp.).

Jarvis I, Murphy AM, Gale AS (2001) Geochemistry of pelagic and hemipelagic carbonates: criteria for identifying systems tracts and sea-level change. J Geol Soc Lond 158:685–696

Kalkreuth W, Kotis T, Papanicolaou C, Kokkinakis P (1991) The geology and coal petrology of a Miocene lignite profile at Meliadi Mine, Katerini. Greece Int J Coal Geol 17:51–67

Khavari Khorasani, G., 1987. Oil-prone coals of the Walloon coal measures, Surat Basin, Australia. In: Scott, A.C. (Ed.), Coal and Coal-Bearing Strata: Recent Advances. Geological Society Special Publication 32 303–310.

Kuder T, Kruge MA, Shearer JC, Miller SL (1998) Environmental and botanical controls on peatification — a comparative study of two New Zealand restiad bogs using Py-GC/MS, petrography and fungal analysis. Int J Coal Geol 37(1–2):3–27

Kumar M, Srivastava G, Spicer RA, Spicer TEV, Mehrotra RC, Mehrotra NC (2012) Sedimentology, palynostratigraphy and palynofacies of the late Oligocene Makum Coalfield, Assam, India: A window on lowland tropical vegetation during the most recent episode of significant global warmth. Palaeogeogr Palaeoclimatol Palaeoecol 342–343:143–162

Lamberson MN, Bustin RM, Kalkreuth W (1991) Lithotype (maceral) composition and variation as correlated with paleowetland environments. Gates Formation, Northeastern British Columbia. Canada Int J Coal Geol 18:87–124

Li Z, Ward CR, Gurba LW (2010) Occurrence of non-mineral inorganic elements in macerals of low-rank coals. Int J Coal Geol 81:242–250

Mallet FR (1876) On the coalfields of the Naga Hills bordering the Lakhimpur and Sibsagar districts. Assam Memoir Geological Survey of India 12(2):269–363

Mathur, L. P. and Evans, P. 1964. Oil in India. 22nd Int. geol. Congr., New Delhi: 1·87.

Mathur N (2014) Tertiary oils from Upper Assam Basin, India: a geochemical study using terrigenous biomarkers. Org Geocemistry 76:9–25

McInerney FA, Wing SL (2011) The Paleocene-Eocene Thermal Maximum: a perturbation of carbon cycle, climate, and biosphere with implications for the future. Annu Rev Earth Planet Sci 39:489–516

McLennan, S.M., 2001. Relationships between the trace element composition of sedimentary rocks and upper continental crust. Geochem. Geophys. Geosyst. 2 (1021).

McLennan SM, Hemming S, McDaniel DK, Hanson GN (1993) Geochemical approaches to sedimentation, provenance, and tectonics. Geol Soc Am Special Pap 284:21–40

Meddlicott HB (1865) The coal of Assam, result of a brief visit to the coalfields of that Province in 1865; with geological notes on Assam and hills to the south of it. Mem Geol Surv India 4(3):388–442

Mendonça Filho, J.G., Carvalho, M.A., Menezes, T.R., 2002. Palinofácies. In: Dutra, T.L. (Ed.), Técnicas e Procedimentos para o Trabalho com Fósseis e Formas Modernas Comparativas. Unisinos, São Leopoldo 20–24.

Mendonça Filho, J.G., Mendonça, J.O., Menezes, T.R., Oliveira, A.D., Carvalho, M.A., Santanna, A.J., Souza, J.T., 2010. Palinofácies. In: Carvalho, I.S. (Ed.), Paleontologia, third ed. 1. Interciência, Rio de Janeiro 379–413.

Mendonça Filho, J.G., Menezes, T.R., Mendonça, J.O., 2011. Organic composition (palynofacies analysis). Chapter 5, ICCP Training Course on Dispersed Organic Matter, pp. 33–81.

Mendonça Filho, J.G., Menezes, T.R., Mendonça, J.O., Oliveira, A.D., Silva, T.F., Rondon, N.F., Da Silva, F.S., 2012. Organic facies: palynofacies and organic geochemistry approaches. In: Panagiotaras, D. (Ed.), Geochemistry – Earth's System Processes. InTech 211–248.

Miller KG, Kominz MA, Browning JV, Wright JD, Mountain GS, Katz ME, Sugarman PJ, Cramer BS, Christie-Blick N, Pekar SF (2005) The phanerozoic record of global sea-level change. Science 310:1293–1298

Mishra HK, Ghosh RK (1996) Geology, petrology and utilisation potential of some Tertiary coals of northeastern region of India. Int J Coal Geol 30:65–100. https://doi.org/10.1016/0166-5162(95)00038-0

Misra BK (1992) Optical properties of some Tertiary coals from northeastern India: their depositional environment and hydrocarbon potential. Int J Coal Geol 20:115–144. https://doi.org/10.1016/0166-5162(92)90007-J

Misra BK (2000) Petrography, genesis and deposition of Tertiary coals from northeastern India. Palaeobotanist 49:177–195

Moore TA, Shearer JC (2003) Peat/coal type and depositional environment—are they related? Int J Coal Geol 56:233–252

Mukhopadhyay PK (1986) Petrography of selected Wilcox and Jackson group Lignites from the Tertiary of Texas. In: Finkelman, R.B., Casagrande, D.J. (Eds.), Geology of Gulf Coast Lignites. 1986 Annual Meeting of Geological Society of America. Field Trip 126–145.

Mukhopadhyay PK, Hatcher PG, Calder JH (1991) Hydrocarbon generation from deltaic and intermontane fluviodeltaic coal and coaly shale from the Tertiary of Texas and Carboniferous of Nova Scotia. Org Geochem 17:765–783

Naidu BD, Panda BK (1997) 'Regional source rock mapping in upper Assam Shelf', Proceedings of the Second International Petroleum Conference and Exhibition, Petrotech-97 1 350–364, New Delhi.

Nesbitt HW, Young GM (1982) Early Proterozoic climates and plate motions inferred from major element chemistry of lutites. Nature 299:715–717

Nesbitt HW, Young GM (1984) Prediction of some weathering trends of plutonic and volcanic rocks based on thermodynamic and kinetic considerations: Geochim. Cosmochim Acta 48:1523–1534

Nesbitt HW, Young GM, McLennan SM, Keays RR (1996) Effects of chemical weathering and sorting on the petrogenesis of siliciclastic sediments, with implications for provenance studies. J Geol 104:525–542

O'Keefe JMK, Hower JC (2011) Revisiting Coos Bay, Oregon: a re-examination of funginite-huminite relationships in Eocene subbituminous coals. Int J Coal Geol 85:34–42

Patterson SH (1971) Investigations of ferruginous bauxite and other mineral resources on Kauai and reconnaissance of ferruginous bauxite deposits on Maui. Hawaii u s Geol Surv Prof Pap 656:74

Peters, K.E., Cassa, M.R., 1994. Applied source rock geochemistry. In: Magoon, L.B., Dow, W.G. (Eds.), The Petroleum System from Source to Trap. AAPG Memoir. 60, 93–120.

Petersen HI, Lindström S, Nytoft HP, Rosenberg P (2009) Composition, peatforming vegetation and kerogen paraffinicity of Cenozoic coals: relationship to variations in the petroleum generation potential (Hydrogen Index). Int J Coal Geol 78:119–134

Pickel, W., Kus, J., Flores, D., Kalaitzidis, S., Christanis, K., Cardott, B.J., Misz-Kennan, M., Rodrigues, S., Hentschel, A., Hamor-Vido, M., Crosdale, P., Wagner, N., ICCP, 2017. Classification of liptinite – ICCP System 1994. Int. J. Coal Geol. 169, 40–61

Querol X, Cabrera L, Pickel W, López-Soler A, Hagemann HW, Fernández-Turiel JL (1996) Geological controls on the coal quality of the Mequinenza subbituminous coal deposit, northeast Spain. Int J Coal Geol 29(1–3):67–91

Raja Rao CS (1981) Coalfields of India; coalfields of northeastern India. Bull Geol Surv India Ser a 1(45):1–76

Rajarathnam S, Chandra D, Handique GK (1996) An overview of chemical properties of marineinfluenced Oligocene coal from the northeastern part of the Assam-Arakan basin. India Int J Coal Geol 29:337–361

Raju ATR (1968) Geological evolution of Assam and Cambay Tertiary basins of India. Bull Am Assoc Pet Geol 52:2422–2437

Raju SV, Mathur N (1995) Petroleum geochemistry of a part of Upper Assam Basin, India: a brief overview. Org Geochem 23(1):55–70

Ranga RA (1983) Geology and hydrocarbon potential of a part of Assam-Arakan and its adjacent region. Petr Asia J 6:127–158

Rice DD, Clayton JL, Pawlewicz MJ (1989) Characterization of coal-derived hydrocarbons and source-rock potential of coal beds, San Juan Basin, New Mexico and Colorado, U.S.A. Int J Coal Geol 13:597–626

Roaldest, E., 1978. Mineralogical and chemical changes during weathering, transportation and sedimentation in different environments with particular references to the distribution of Ytrium and lanthanide elements. Ph.D. Thesis, Geol. Inst., Univ. of Oslo, Norway.

Roser BP, Korsch RJ (1986) Determination of tectonic setting of sandstone mudstone suites using SiO2 content and K2O/Na2O ratio. J Geol 94:635–650

Roser BP, Korsch RJ (1988) Provenance signatures of sandstone-mudstone suites determined using discriminant function analysis of major-element data. Chem Geol 67:119–139

Rudnick RL, Gao S (2004) Composition of the continental crust. Treatise Geochem 3:1–64

Rudra A, Dutta S, Raju SV (2017) The Paleogene vegetation and petroleum system in the tropics: A biomarker approach. Mar Pet Geol 86:38–51

Saikia BK, Saikia A, Choudhury R, Xie P, Liu J, Das T, Dekaboruah HP (2016) Elemental geochemistry and mineralogy of coals and associated coal mine overburden from Makum coalfield (Northeast India). Environmental Earth Sciences 75(8):1–21

Saikia BK, Ward CR, Oliveira MLS, Hower JC, Baruah BP, Braga M, Silva LF (2014) Geochemistry and nanomineralogy of two medium-sulfur northeast Indian coals. Int J Coal Geol 121:26–34

Saikia BK, Ward CR, Oliveira MLS, Hower JC, Leao FD, Johnston MN, O'Bryan A, Sharma A, Baruah BP, Silva LFO (2015) Geochemistry and nano- mineralogy of feed coals, mine overburden, and coal-derived fly ashes from Assam (North-east India): a multi-faceted analytical approach. Int J Coal Geol 137:19–37

Schouten S, Woltering M, Rijpstra WIC, Sluijs A, Brinkhuis H, Damsté JSS (2007) The Paleocene-Eocene carbon isotope excursion in higher plant organic matter: differential fractionation of angiosperms and conifers in the Arctic. Earth Planet Sci Lett 258:581–592

Scott AC (2002) Coal petrology and the origin of coal macerals: a way ahead? Int J Coal Geol 50:119–134

Shalaby MR, Osli LN, Kalaitzidis S, Islam MA (2019) Thermal maturity and depositional palaeoenvironments of the Cretaceous-Palaeocene source rock Taratu formation, Great South Basin. New Zealand. J Pet Sci Eng 181:106156

Shanmugam G (1985) Significance of coniferous rain forests and related organic matter in generating commercial quantities of oil, Gippsland Basin, Australia. Am Asso Petrol Geol Bull 69:1241–1254

Sharma A, Phukan S, Saikia BK, Baruah BP (2018) Geochemical evaluation of the hydrocarbon prospects of carbonaceous shale and coal of Barail Group, Upper Assam Basin. International Journal of Oil, Gas and Coal Technology 19(3):263–282

Shehata, M.G., Abdou, A.A., 2008. Geochemical study of the shale of Gebel El – dist Member, Bahariya Oasis, Western deser, Egypt., Australian Journal BAS 2(2) 243–251.

Silva LFO, Oliveira MLS, Neace ER, O'Keefe JMK, Henke KR, Hower JC (2011a) Nanominerals and ultrafine particles in sublimates from the Ruth Mullins coal fire, Perry County, Eastern Kentucky, USA. Int J Coal Geol 85:237–245

Silva LFO, Querol X, da Boit KM, Fdez-Ortiz de Vallejuelo S, Madariaga JM (2011b) Brazilian coal mining residues and sulphide oxidation by Fenton's reaction: an accelerated weathering procedure to evaluate possible environmental impact. J Hazard Mater 186:516–525

Silva MB, Kalkreuth W (2005) Petrological and geochemical characterization of Candiota coal seams, Brazil — implication for coal facies interpretations and coal rank. Int J Coal Geol 64:217–238

Singh AK, Kumar A (2017) Petro-chemical characterisation and depositional paleoenvironment of lignite deposits of Nagaur, Western Rajasthan. India Environmental Earth Sciences 76(20):1–18

Singh MP, Singh AK (2000) Petrographic characteristics and depositional conditions of Eocene coals of platform basins, Meghalaya. India Int J Coal Geol 42:315–356

Snowdon LR (1991) Oil from Type III organic matter: resinite revisited. Org Geochem 17:743–747

Srivastava G, Spicer RA, Spicer TEV, Yang J, Kumar M, Mehrotra R, Mehrotra N (2012) Megaflora and palaeoclimate of a Late Oligocene tropical delta, Makum Coalfield, Assam: evidence for the early development of the South Asia Monsoon. Palaeogeogr Palaeoclimatol Palaeoecol 342–343:130–142

Stach, E., Mackowsky, M.Th., Teichmiiller, M., Tayler, G.H., Chandra, D. and Teichmiiller, R., 1982. Stach's Textbook of Coal Petrology. Borntraeger, Berlin, 3rd ed 535

Suárez-Ruiz I, Deolinda F, Filho JGM, Hackley PC (2012) Review and update of the applications of organic petrology: Part 2, geological and multidisciplinary applications. Int J Coal Geol 98:73–94

Sykes R, Volk H, George SC, Ahmed M, Higgs KE, Johansen PE, Snowdon LR (2014) Marine influence helps preserve the oil potential of coaly source rocks: Eocene Mangahewa Formation, Taranaki Basin, New Zealand. Org Geochem 66:140–163

Taylor, G.H., Teichmüller, M., Davis, A., Diessel, C.F.K., Littke, R., Robert, P., 1998. Org. Petrol 16. Gerbrüder Borntraeger, Berlin 704.

Teichmüller M (1989) The genesis of coal from the viewpoint of coal petrology. Int J Coal Geol 12:1–89

Thomas BM (1982) Land – plant source rocks for oil and their significance in Australian Basins. Australian Petroleum Exploration Association Journal 22:164–178

Thompson S, Cooper BS, Morley RJ, Barnard PC (1985) Oil generating coals. In: Thomas BM et al (eds) Petroleum Geochemistry in Exploration of the Norwegian Shelf. Graham and Trotman, London, pp 59–73

Tissot BP, Welte DH (1978) Petroleum Formation and Occurrence. Springer, New York

Traverse A (1988) Paleopalynology. Unwin Hyman, London, p 600

Tyson RV (1995) Sedimentary Organic Matter. Organic Facies and Palynofacies. Chapman & Hall, London, p 615

Varma AK, Biswas S, Patil JD, Mani D, Misra S, Hazra B (2019) Significance of lithotypes for hydrocarbon generation and storage. Fuel 235:396–405. https://doi.org/10.1016/j.fuel.2018.07.111

Veizer J, Demovic R (1974) Strontium as a tool in facies analysis. J Sediment Res 44:93–115

Ward CR (1991) Mineral matter in low-rank coals and associated strata of the Mae Moh Basin, northern Thailand. Int J Coal Geol 17:69–93

Ward CR (2002) Analysis and significance of mineral matter in coal seams. Int J Coal Geol 50:135–168

Wüst RAJ, Hawke MI, Bustin RM (2001) Comparing maceral ratios from tropical peat lands with assumptions from coal studies: do classic coal petrographic interpretation methods have to be discarded? Int J Coal Geol 48:115–132

Xiao WJ, Han CM, Yuan C, Sun M, Lin SF, Chen HL, Li ZL, Li JL, Sun S (2008) Middle Cambrian to Permian subduction-related accretionary orogenesis of Northern Xinjiang, NW China: implications for the tectonic evolution of central Asia. J Asian Earth Sci 32:102–117

Yu Y, Zhang CM, Li SH, Zhu R, Du JY, Wang L (2014) Geochemical characteristics and geological significance of mudstones from Zhujiang formation of Huizhou depression. J China Univ Pet 38(1):40–49

Zhao L, Dai S, Graham IT, Li X, Liu H, Song X, Hower JC, Zhou Y (2017) Cryptic sediment-hosted critical element mineralization from eastern Yunnan Province, southwestern China: mineralogy, geochemistry, relationship to Emeishan alkaline magmatism and possible origin. Ore Geol Rev 80:116–140